Session 3

NOBLE GAS SEPARATION

MONDAY: October 20, 1980
CHAIRMAN: Clifford Burchsted
Oak Ridge National Laboratory

REVIEW OF THE ADSORPTION OF RADIOACTIVE KRYPTON AND XENON ON ACTIVATED CHARCOAL

Dwight W. Underhill, Sc.D.
Associate Professor,
Graduate School of Public Health
University of Pittsburgh

and

Dade W. Moeller, Ph.D.
Chairman, Department of Environmental
Health Sciences
School of Public Health
Harvard University

Abstract

This report summarizes the results of a critical review of the published literature on the adsorption of radioactive krypton and xenon on activated charcoal. This review, which was supported by the Advisory Committee on Reactor Safeguards, U. S. Nuclear Regulatory Commission, showed that (a) individual charcoals have a wide range of adsorption coefficients and therefore the performance of a given bed is heavily dependent on the quality of the charcoal it contains; (b) because of the detrimental effects of mass transfer on noble gas adsorption, consideration should be given to including this factor in developing technical specifications for adsorption beds; and (c) additional research is needed on the determination of the inter-relationship of moisture and temperature and their effects on adsorption bed performance.

I. Introduction

Most of the radionuclide releases from operating nuclear power plants are in the form of airborne krypton and xenon. The standard procedure for handling such discharges is the use of charcoal delay beds, so that the shorter lived radioisotopes of these two gases can decay before being released to the ambient atmosphere. Because a detailed understanding of the performance of such beds is important during routine as well as accident conditions, as well as in the application of the ALARA criterion to this type of engineered safety feature, the Advisory Committee on Reactor Safeguards, U. S. Nuclear Regulatory Commission, supported in 1979 an indepth review of all the published scientific data on this subject. The results of this review were published as NUREG-0678.[1] The purpose of this paper is to bring to the attention of participants in this Nuclear Air Cleaning Conference the results of this effort and to highlight some of our findings.

II. Adsorption Coefficients for Krypton and Xenon

Measurements of the adsorption coefficients for krypton and xenon on activated charcoal have been made in a number of countries, including the United States, England, Italy, Japan, the Federal Republic of Germany, the German Democratic Republic, the Soviet Union,

and Czechoslovakia. Because the information from these studies remained scattered in various journals and reports (some of which are difficult to obtain), a major effort was made to assemble these data in a manner that would permit critical evaluation. As an initial approach, the reported adsorption coefficients were grouped according to the noble gas (either krypton or xenon) and according to the carrier gas. For some combinations of noble gas - carrier gas, a large number of test results were located. For example, for the adsorption of krypton and xenon from air, 75 and 44 separate pieces of data were located, respectively. Other combinations of noble gas-carrier gas were not as well represented. For the adsorption of krypton and xenon from oxygen, for example, only 18 data points could be located for the former and none for the latter.

As is well known, the adsorption coefficient is strongly dependent on the temperature at which the test was made. In order to permit calculations of the adsorption coefficient at intermediate temperatures, these data were fitted to a temperature dependent equation. The equation chosen for this purpose was that developed by Antoine[2]

$$k = e^{\left(A + \frac{B}{C + T}\right)} \qquad (1)$$

where:

k = adsorption coefficient, cc(NTP)/gm
A,B, and C = constants for the Antoine equation
T = temperature in °C

The geometric standard deviation, σ, between the observed and estimated adsorption coefficients was determined using the equation:

$$\ln(\sigma) = \sqrt{\frac{\Sigma_\eta \left[\ln(k_i) - \ln(k_i')\right]^2}{\eta - 3}} \qquad (2)$$

where:

k_i' = the estimate of the i^{th} data point, k_i.

The results of this analysis for each combination of noble gas-carrier gas are given in Table 1. Values of the adsorption coefficients determined from the Antoine equation are shown in Figures 1 and 2.

The Antoine equation has been used primarily for calculating the vapor pressure of liquids, and it is thought that this is the first time that it has been applied to correlate the adsorption coefficients for radioactive krypton and xenon. Nonetheless it would be expected that this equation would be well suited to this purpose because adsorption is in many ways comparable to liquefaction and the adsorption coefficient can be looked upon as being the reciprocal of a vapor pressure.

When the Antoine equation was applied to the available data for the adsorption of krypton and xenon from hydrogen, the geometric

standard deviations were 2% and 6%, respectively. This excellent result is no doubt due in part to the fact that all the available data were from the same laboratory and from experiments using only one grade of charcoal. When data from many laboratories, obtained using various experimental equipment, and perhaps, more importantly, different charcoals, were correlated by means of the Antoine equation, the geometric standard deviations were considerably higher. For example, the geometric standard deviations for the adsorption of krypton and xenon from air were 37% and 44%, respectively.

The wide range in the adsorption coefficients for krypton and xenon from air is illustrated in Figures 3 and 4. Although the curves in the figures are not intended to be used as sources of specific numbers, the calculations used to develop the data used in plotting them showed that, at 25°C, the adsorption coefficient for krypton from dry air was estimated to be less than 22 cc(NTP)/gm for 5%, and less than 72 cc(NTP)/gm for 95%, of the charcoals tested. In this regard, it is worth noting that a value of 70 cc(NTP)/gm, suggested by Cardile and Bellamy,[3] has been used as an estimate of the adsorption coefficient for krypton under these same conditions. Although this value could probably be surpassed by a number of commercial charcoals, it is significantly higher than the mean value of 40 cc(NTP)/gm found here. A similar observation was made regarding the adsorption coefficient for xenon.

The above example illustrates that there is no single correct value for the adsorption coefficient for either krypton or xenon at a given temperature. Instead, there is a range of values and the particular value observed will depend, in part, on the quality of the charcoal used. From the standpoint of safety analysis, it is unwise to assume specific values for the adsorption of either krypton or xenon without having confirming data for the particular charcoal to be employed at the same temperature and with the carrier gas to be used in the system under consideration.

III. Significance of Moisture

This review showed that moisture can severely interfere with the adsorption of krypton and xenon on charcoal. Three references reported reductions in the adsorption coefficient for krypton of between 6% and 10% for each 1% adsorbed water (by weight) in the range of 0% to 2% adsorbed water. As the quantity of adsorbed water increased over 5%, there was a reduction in the percent decrease for each additional percent of adsorbed water. Although the rate of decrease was smaller at higher water contents, the data showed that the accumulative effect can be severe. One author[4] observed a 90% reduction in the adsorption coefficient for krypton as the water content of the charcoal increased from 0% to 35% (by weight).

Because of the limited amount of data on the effects of adsorbed water on the adsorption of xenon, it was not possible to make any general correlations. This is unfortunate for two reasons. First, the xenon adsorption coefficient may be more influenced by adsorbed water than the krypton adsorption coefficient; second, in adsorption beds operating at room temperature, it is generally the

xenon radioisotopes that have the higher effluent activity.

Also noted in this review was the high degree of scatter in the experimental results reported on the effects of adsorbed water. This scatter may be a consequence of the long time required to bring a sample of activated charcoal into equilibrium with an incoming stream of air with a fixed relative humidity. In NUREG-0678[1], experimental procedures are suggested which, if followed, should reduce the experimental error in such measurements.

This review showed that only fragmentary data were available on the effect of adsorbed water on the adsorption coefficients for either krypton or xenon at temperatures other than ambient. From the standpoint of noble gas adsorption systems, there appears to be an inadequate data base, as well as the absence of an established procedure to expand this base, relative to the effects of adsorbed water on the adsorption coefficients of krypton and xenon.

IV. Effects of Pressure

The effects of pressure on the adsorption of krypton and xenon were correlated in terms of a dimensionless factor, α, which is called here the pressure coefficient. This coefficient is defined as:

$$\alpha = \frac{k_2 - k}{k \ell n P_2} \qquad (3)$$

where α = Pressure Coefficient, dimensionless
k = Adsorption Coefficient at 1 Atm(Abs), cc(NTP)/gm
k_2 = Adsorption Coefficient at Pressure, P(Abs), cc(NTP)/gm

If both the pressure coefficient, α, and the adsorption coefficient, k, at atmospheric pressure, are known, then the adsorption coefficient, k_2, at a pressure, P_2, can be determined directly from α and k using Equation 3. Values for α for both krypton and xenon are plotted in Figure 5 as a function of temperature. From this Figure, it may be noted that a change in temperature has a significant impact on the effects of pressurization. It is also apparent that, for a given temperature, an increase in pressure is more effective in increasing the adsorption coefficient for krypton than for xenon.

Another important observation is that the relative effectiveness of pressurization decreases as the temperature is reduced. For example, at 25 °C, raising the pressure from 1 to 10 atmospheres (abs) will increase the adsorption coefficient by a factor of 4.2 for krypton and by a factor of 3.8 for xenon. At -50°C, the same increase in pressure will increase the adsorption coefficient for kryton by only a factor of 2.4 and for xenon by a factor of only 1.45.

From the standpoint of nuclear air cleaning, it is important to know that the fractional increase in the adsorption coefficient, even at room temperature, is considerably less than the fractional

increase in absolute pressure. Furthermore, it is important to note that, at reduced pressure, the effectiveness of pressurization is reduced still further.

V. Effect of Noble Gas Concentration

Some people have questioned whether the adsorption coefficients for krypton and xenon on activated charcoal might be significantly reduced at high concentrations. If this were so, then adsorption beds could be rendered ineffective by the high concentrations of krypton and xenon that might occur in an unexpected release -- the very time that effective performance of such beds is most needed.

By far the most extensive data on this subject are those reported by Collins et al.[5] for the adsorption of krypton and xenon from an argon carrier gas. Using these data, it is possible to calculate the coefficients for the Langmuir equation:

$$k_3 = k/(1+ C_1/\bar{C}_1 + C_2/\bar{C}_2) \qquad (4)$$

where k_3 = adsorption coefficient for xenon (krypton) at increased krypton and/or xenon concentrations, cc(NTP)/gm

k = adsorption coefficient of xenon (krypton) at infinitely low xenon and krypton concentrations, cc(NTP)/gm

C_1 = concentration of xenon (krypton), ppm

$\bar{C}_1$ = Langmuir coefficient for the effect of xenon (krypton) concentration on the adsorption of xenon (krypton), ppm

C_2 = concentration of krypton (xenon), if present, ppm

$\bar{C}_2$ = Langmuir coefficient for the effect of the krypton (xenon) concentration on the adsorption of xenon (krypton), ppm

Values for the Langmuir coefficients as calculated on this basis are summarized in Table 2.

Comparison of the data published by Collins et al. [5] and those derived by the Langmuir equation show that the geometric standard deviation between the measured and the predicted adsorption coefficients was 1.11 and 1.19, respectively, for the adsorption of krypton in the absence of xenon and for the adsorption of xenon in the absence of krypton. For the adsorption of xenon from argon that contained appreciable concentrations of krypton, the geometric standard deviation between the measured and predicted values was 1.16.

The effects of high concentrations of noble gases on adsorption coefficients can be calculated directly from the Langmuir coefficients given in Table 2. Sample calculations show that at 20 ^{o}C, for the adsorption coefficients of krypton and xenon to be reduced by 10%, their respective concentrations (by volume) would have to be 10% and 0.5%. These are exceedingly high concentrations. At lower

temperatures, however, the effects of concentration would be more severe. At -50 °C, for example, the adsorption coefficients for krypton and xenon would be reduced by 10% at concentrations (by volume) of 2% and 0.03%, respectively.

Although the above calculations indicate that rather large concentrations of noble gases can be tolerated without degrading holdup bed performance, these estimates omit consideration of the cross interferences between krypton and xenon. From the data in Table 2, it can be seen that the krypton concentration has a significantly greater effect on the adsorption of xenon than it does on itself. Unfortunately, similar data on the effect of the xenon concentration on the adsorption of krypton do not appear to be available. Measurements of this latter effect are especially needed relative to problems of nuclear air cleaning since the fission yield of xenon is greater than that of krypton. To provide noble gas holdup bed designers with the data they need to solve these and related problems, it is recommended that the following specific studies be conducted:

(1) The experiments by Collins et al.[5] be repeated with air as the carrier gas; this will provide data to establish the validity of these data for estimating the adsorption of krypton and xenon from air.
(2) Measurements be undertaken to determine the effect of high xenon concentration on the adsorption of krypton.
(3) Calculations be made of the maximum possible effect that a pulse release of noble gases could have on the holdup of krypton and xenon in operating charcoal beds.

VI. Effects of Mass Transfer

Theory predicts that in most cases the adsorption coefficient is independent of carrier gas velocity.[6] Except for studies conducted at the Brookhaven National Laboratory,[7-9] and elsewhere,[10,11] this theory has been supported by experimental data. Mass transfer, however, does affect the decontamination factor. This effect is due to the random distribution of the velocities of the noble gas atoms which causes some of them to be retained longer than others. As a result, even if a pulse of radioactive gas is injected into an adsorption bed, there will be a spread in the concentrations of the gas as it leaves the bed (Figure 6). Fortunately, this spreading effect can be correlated satisfactorily using the van Deemter equation[12] and the radionuclide concentrations in the effluent stream calculated as follows. Using one of the methods outlined in Figure 6, the number of theoretical plates is calculated. Following this, the effects of mass transfer on the decontamination factor can be determined from Figures 7 and 8, which were developed for interparticle and intraparticle diffusion, respectively. As a rule of thumb, Figure 7 is preferred if the Peclet number for the carrier gas velocity is below unity. It is noteworthy that for more than 50 theoretical plates, Figures 7 and 8 give essentially the same results.

VII. Commentary

In the design of noble gas retention systems, the goal should

be to maintain an acceptable holdup time for the specific radionuclides being released. This review has shown that non-critical acceptance of adsorption coefficients obtained from the published literature can lead to considerable error both in the design and the expected performance of such systems. Through the data provided here and in NUREG-0678,[1] those responsible for such systems have been provided with a range of acceptable values for adsorption coefficients under a variety of operating conditions. This should enable them to estimate in advance what type of performance should be possible as well as reasonable to expect. This, in turn, should lead to the design of adsorption systems that will provide not only better, but also more reliable, performance. Knowledge of the degree of variability of charcoal adsorbents for the retention of krypton and xenon can also assist regulatory agencies, such as the NRC, in establishing more meaningful and realistic testing requirements to assure the adequate performance of such systems.

Acknowledgments

The authors gratefully acknowledge the support of the Advisory Committee on Reactor Safeguards, U. S. Nuclear Regulatory Commission, in the preparation of this report.

References

1. Underhill, D. W., and Moeller, D. W.,"The Effects of Temperature, Moisture, Concentration, Pressure and Mass Transfer on the Adsorption of Krypton and Xenon on Activated Carbon," Report NUREG-0678, Advisory Committee on Reactor Safeguards, U. S. Nuclear Regulatory Commission, Washington, D. C. (July, 1980).

2. Antoine, Ch., "Thermodynamique: Tensions des vapeurs: Nouvelle relation entre les tensions et les temperatures," Comptes Rendus Hebdomadaires des Seances del'Academie des Sciences, 107: 681-684 (1888).

3. Cardile, F. P., and Bellamy, R.R., "Calculation of Releases of Radioactive Materials in Gaseous and Liquid Effluents from Boiling Water Reactors (BWR-Gale Code)," Report NUREG-0016, Revision 1, U. S. Nuclear Regulatory Commission, Washington, D. C. (1979).

4. Foerster, K.,"Delaying Radioactive Fission Product Inert Gases in Cover Gas and Offgas Streams of Reactors by Means of Activated Charcoal Delay Lines," Kerntechnik, 13: 214-219 (1971).

5. Collins, D. A., Taylor, R., and Taylor, R. L., "The Adsorption of Krypton and Xenon from Argon by Activated Charcoal," AERE Report TRG-1578 (W) (1967).

6. Lovell, R., and Underhill, D. W., "Experimental Determination of Fission Gas Adsorption Coefficients," Report CONF-740807, U. S. Energy Research and Development Administration, pp 893-900 (1979).

7. Wirsing, E., Jr., Hatch, L. P., and Dodge, B. F., "Low Temperature Adsorption of Krypton on Solid Adsorbents," Report BNL-50254 (T-586), U. S. Atomic Energy Commission, Washington, D. C. (1970).

8. Kenney, W. F., and Eshaya, A. M., "Adsorption of Xenon on Activated Charcoal," U. S. Atomic Energy Commission Report BNL - 689 (T-235) (1960).

9. Eshaya, A. M. and Kalinowski, W. L., "Adsorption of Krypton and Mixed Xenon and Krypton on Activated Charcoal," U. S. AEC Report BNL-724 (T-258) (1961).

10. Koch, R. C. and Grandy, G. L., "Retention Efficiencies of Charcoal Traps for Fission Gases," U. S. AEC Report NSEC-7 (1957).

11. Khan, A. A., Deshingkar, D. S., Ramarathinam, K., and Kishore, A. G., "Evaluation of Activated Charcoal for Dynamic Adsorption of Krypton and Xenon," Bhabha Atomic Research Centre (Bombay, India), Report BARA-839 (1976).

12. van Deemter, J. J., Zuiderweg, F. J., and Klinkenberg, A., "Longitudinal Diffusion and Resistance to Mass Transfer as Causes of Non-ideality in Chromatography," Chem. Eng. Sci., Vol. 5, pp. 271-289 (1956).

TABLE 1

Antoine Coefficients for the Adsorption of Krypton and Xenon

System (Adsorbed Gas - Carrier Gas)	Antoine Coefficients			Natural Logarithm of the Geometric Standard Deviation $/\overline{\ln(\sigma)}/$	Number of Data Points (n)	Temperature Range Over Which Data Were Taken (^{o}C)
	A	B	C			
Kr-H_2	-3.56769	1902.38190	240.58930	0.02	10	-40 to 50
Kr-He	-5.06934	3647.85210	332.05548	0.29	44	-120 to 100
Kr-N_2	-9.29824	7963.78580	570.95524	0.25	29	-120 to 25
Kr-Air	-4.68315	3480.87430	391.32352	0.37	75	-150 to 60
Kr-O_2	-0.05476	419.06211	31.63314	0.18	18	0 to 100
Kr-Ar	-19.96366	21305.31700	862.32458	0.26	26	-160 to 38
Kr-CO_2	2.5936	21.50027	36.19603	0.11	9	0 to 60
Xe-H_2	-0.29532	1335.6667	182.50466	0.06	6	0 to 50
Xe-He	-2.57534	2284.49540	227.26565	0.37	45	-80 to 100
Xe-N_2	2.76102	871.51530	202.41475	0.04	6	-20 to 25
Xe-Air	-11.38411	10084.10400	542.88012	0.44	44	-80 to 60
Xe-Ar	-18.49801	16375.16900	622.35258	0.17	29	-100 to 60
Xe-CO_2	1.44594	673.45167	181.85625	0.12	8	0 to 60

TABLE 2
Langmuir Coefficients for the Adsorption of Krypton and Xenon from Argon as Calculated from Data by Collins, et al. (1967)

Temperature (°C)	Langmuir Coefficients for the Effects of the		
	Krypton Concentration on the Adsorption of Krypton	Xenon Concentration on the Adsorption of Xenon	Krypton Concentration on the Adsorption of Xenon
-70	129,000	1,055	28,000
-60	173,000	1,800	49,000
-50	228,000	3,100	81,000
-40	290,000	5,000	125,000
-30	370,000	7,900	185,000
-20	470,000	12,000	262,000
-10	580,000	18,000	360,000
0	710,000	26,000	480,000
10	850,000	37,000	617,000
20	1,020,000	51,000	780,000
30	1,200,000	70,000	
40	1,410,000	93,000	
50	1,640,000	160,000	
60	1,910,000	210,000	

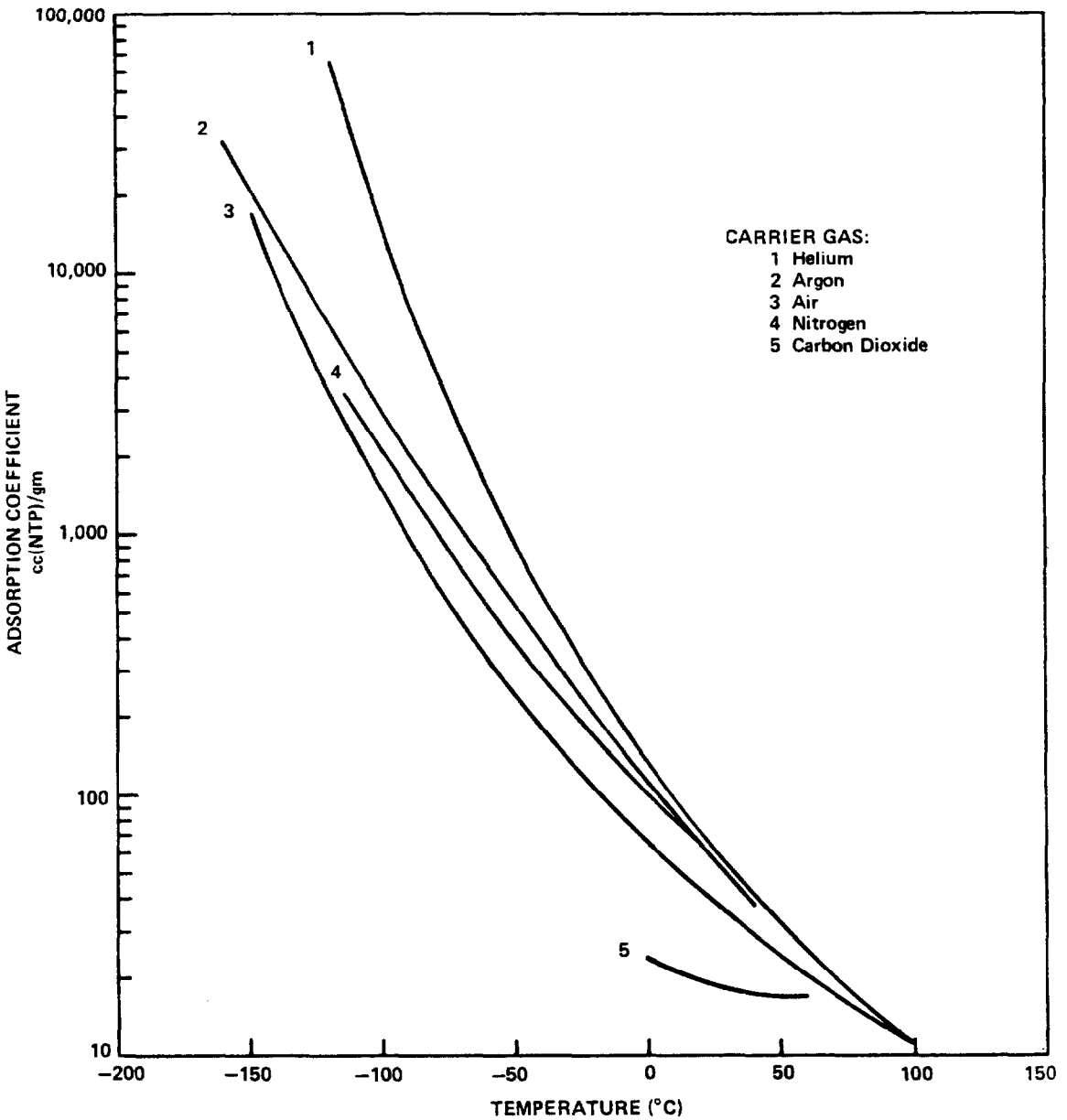

Figure 1 Effect of temperature and carrier gas on the adsorption of krypton.

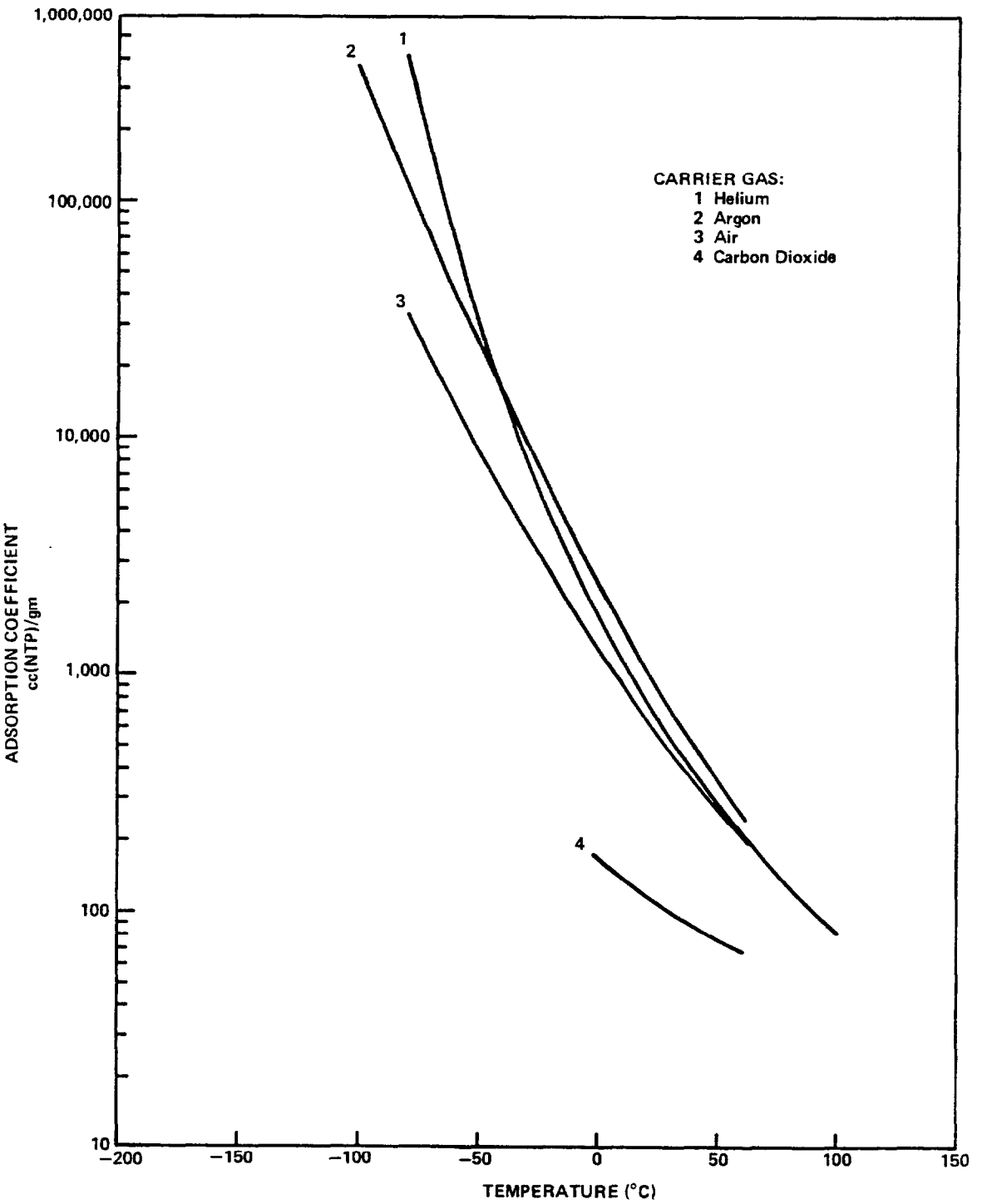

Figure 2 Effect of temperature and carrier gas on the adsorption of xenon.

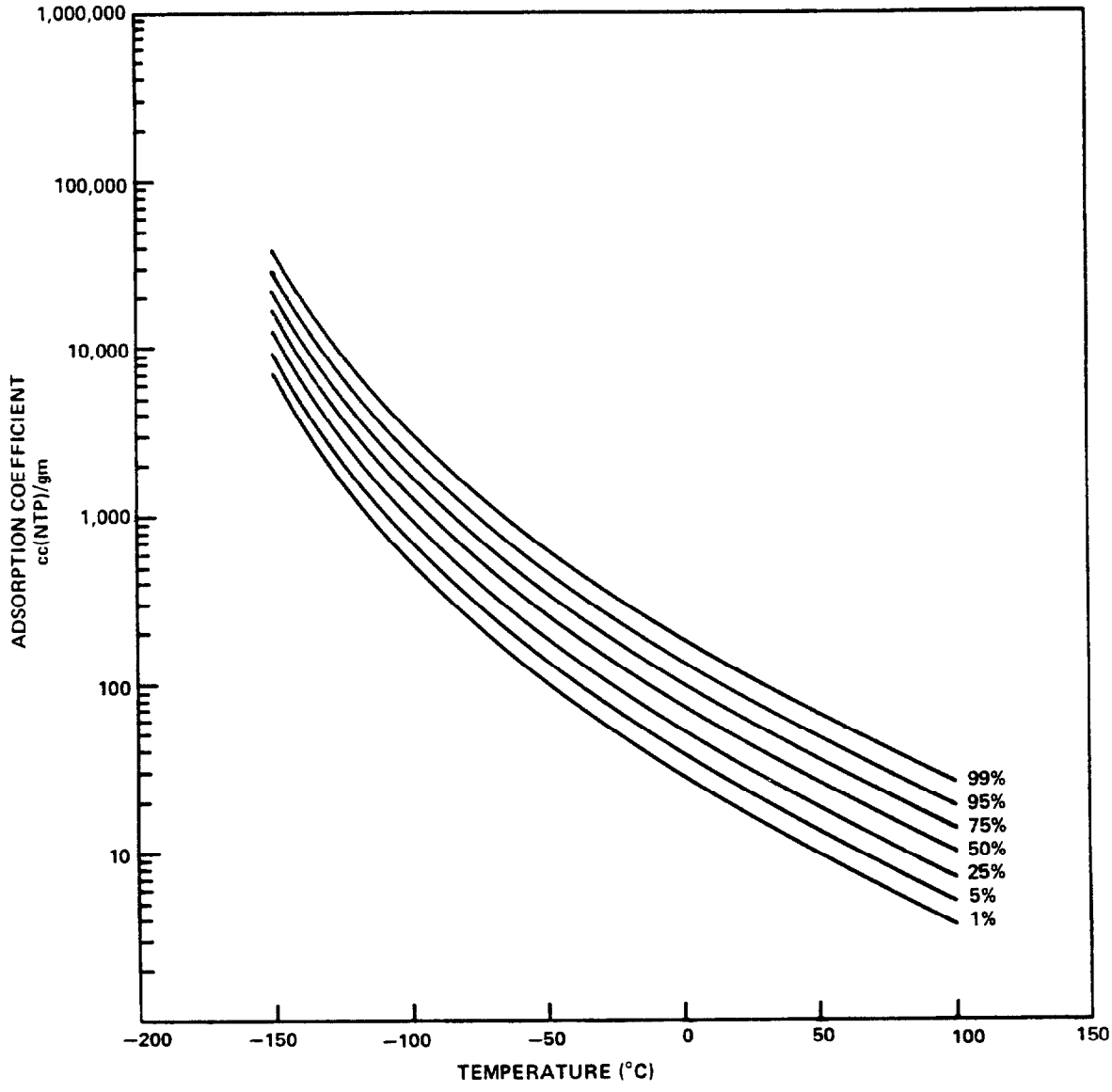

Figure 3 Adsorption of krypton from air: percent of adsorption coefficients expected to be less than stated value.

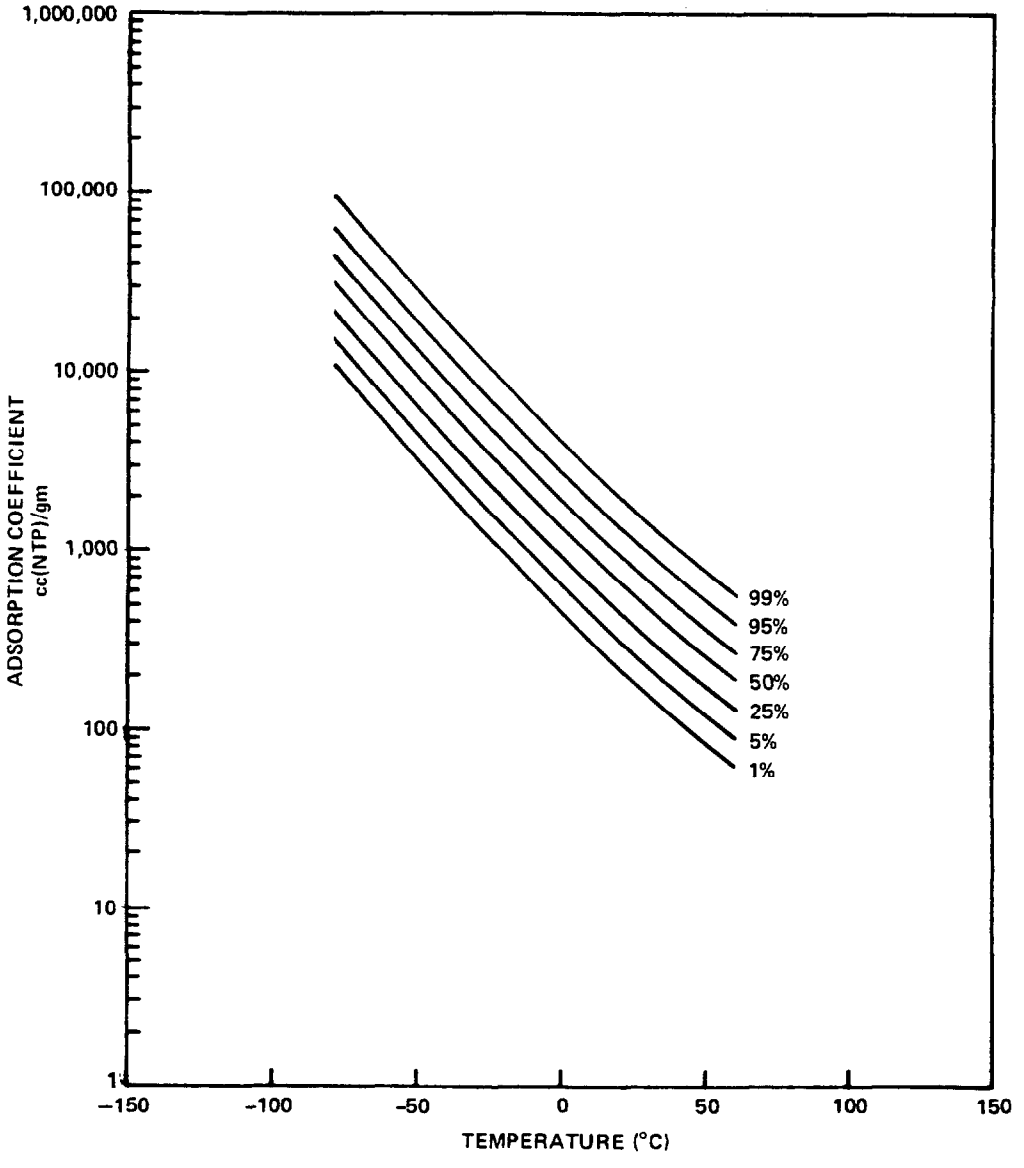

Figure 4 Adsorption of xenon from air: percent of adsorption coefficients expected to be less than stated value.

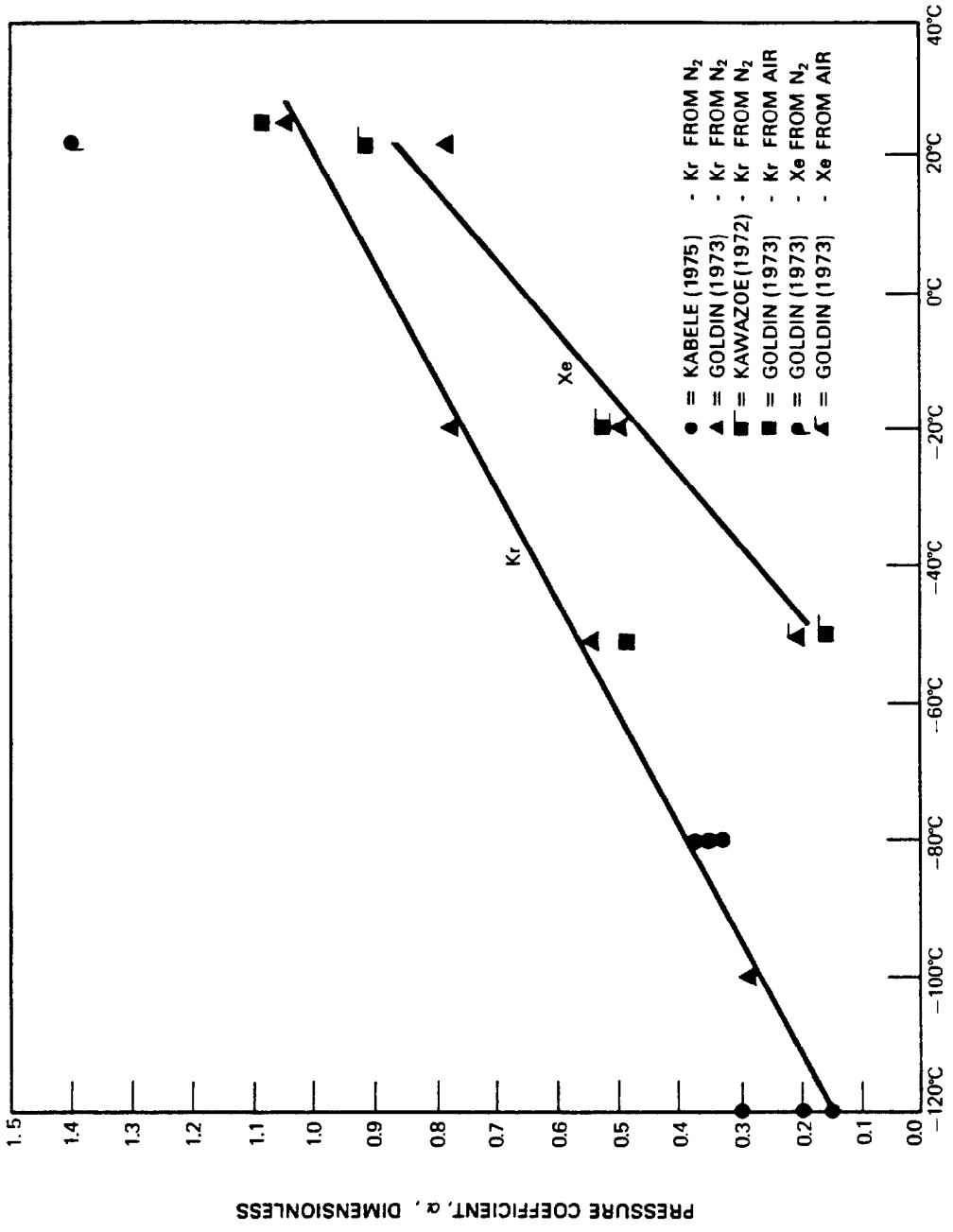

Figure 5 Coefficients for the effect of pressure on the adsorption of krypton and xenon from nitrogen and air.

METHOD #1

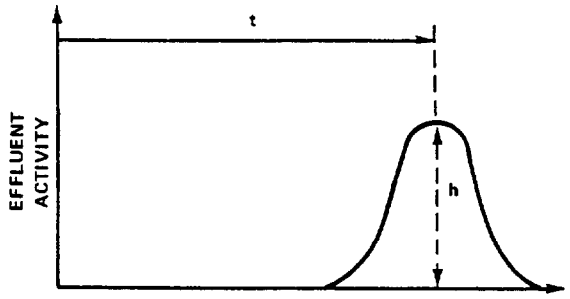

ACCORDING TO THIS METHOD: $N = 2\pi\left(\frac{ht}{A}\right)^2$

WHERE
A = AREA UNDER PEAK
h = HEIGHT OF PEAK
t = TIME AT WHICH EFFLUENT CONCENTRATION OF FISSION GAS REACHES A MAXIMUM

METHOD #2

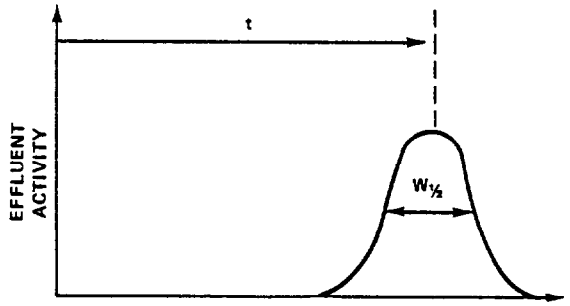

ACCORDING TO THIS METHOD: $N = 5.54\left(\frac{t}{W_{\frac{1}{2}}}\right)^2$

WHERE
$W_{\frac{1}{2}}$ = WIDTH OF PEAK AT HALF HEIGHT

METHOD #3

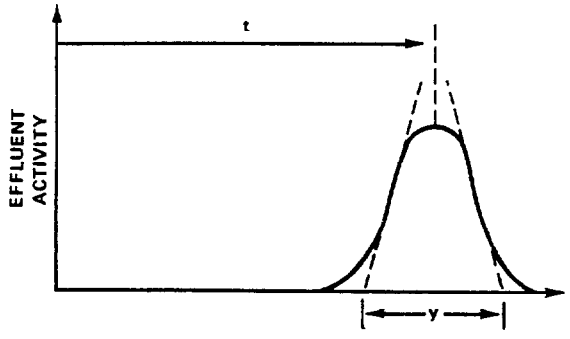

ACCORDING TO THIS METHOD: $N = 16\left(\frac{t}{y}\right)^2$

WHERE
y = WIDTH OF PEAK AT BASE AS DESCRIBED BY LINES DRAWN TO POINT OF INFLECTION (WHERE THE CURVE IS THE STRAIGHTEST)

Figure 6 Three methods of determining the number (N) of theoretical plates from Gaussian breakthrough curves.

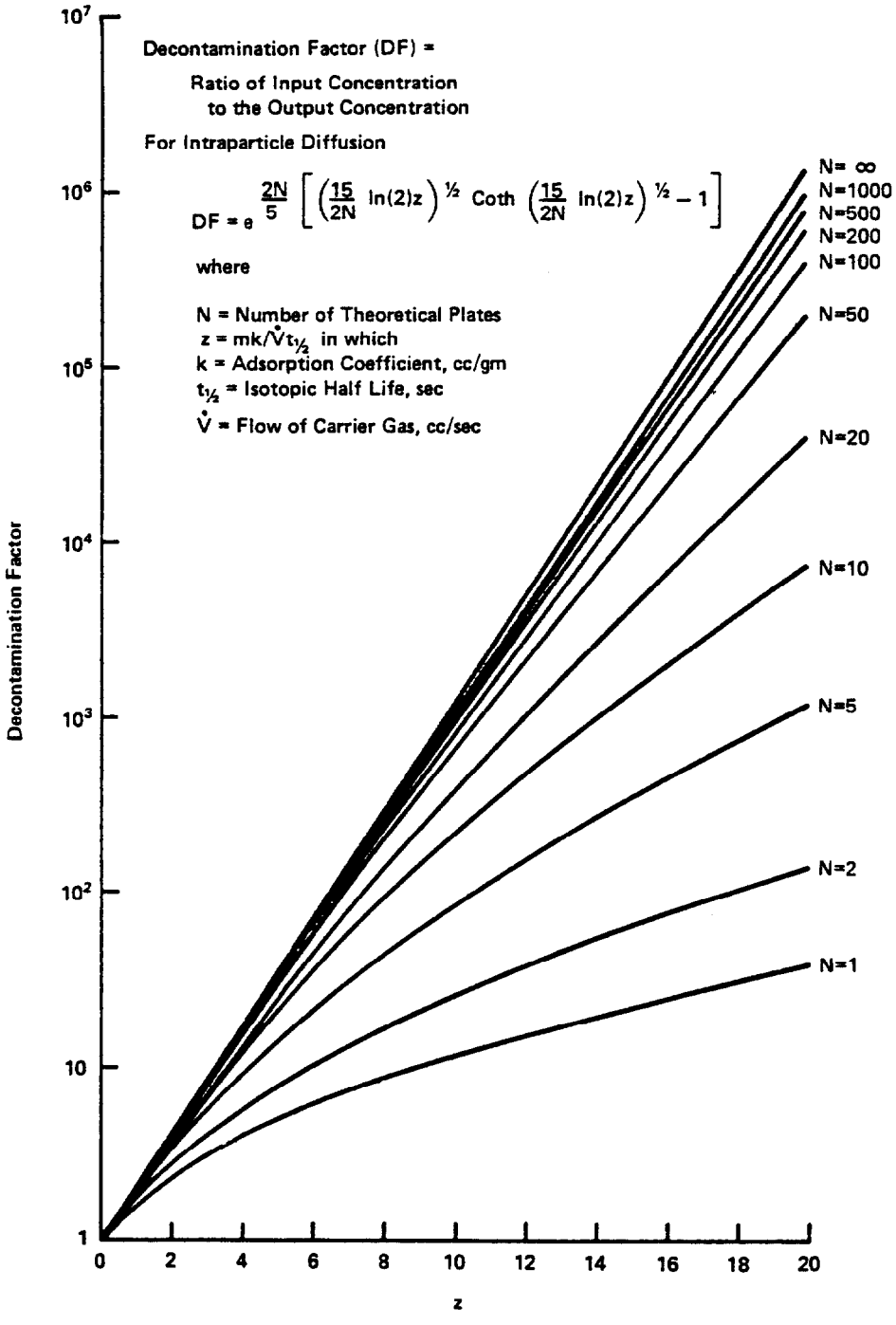

Figure 7 Effect of Intraparticle Diffusion on the Decontamination Factor

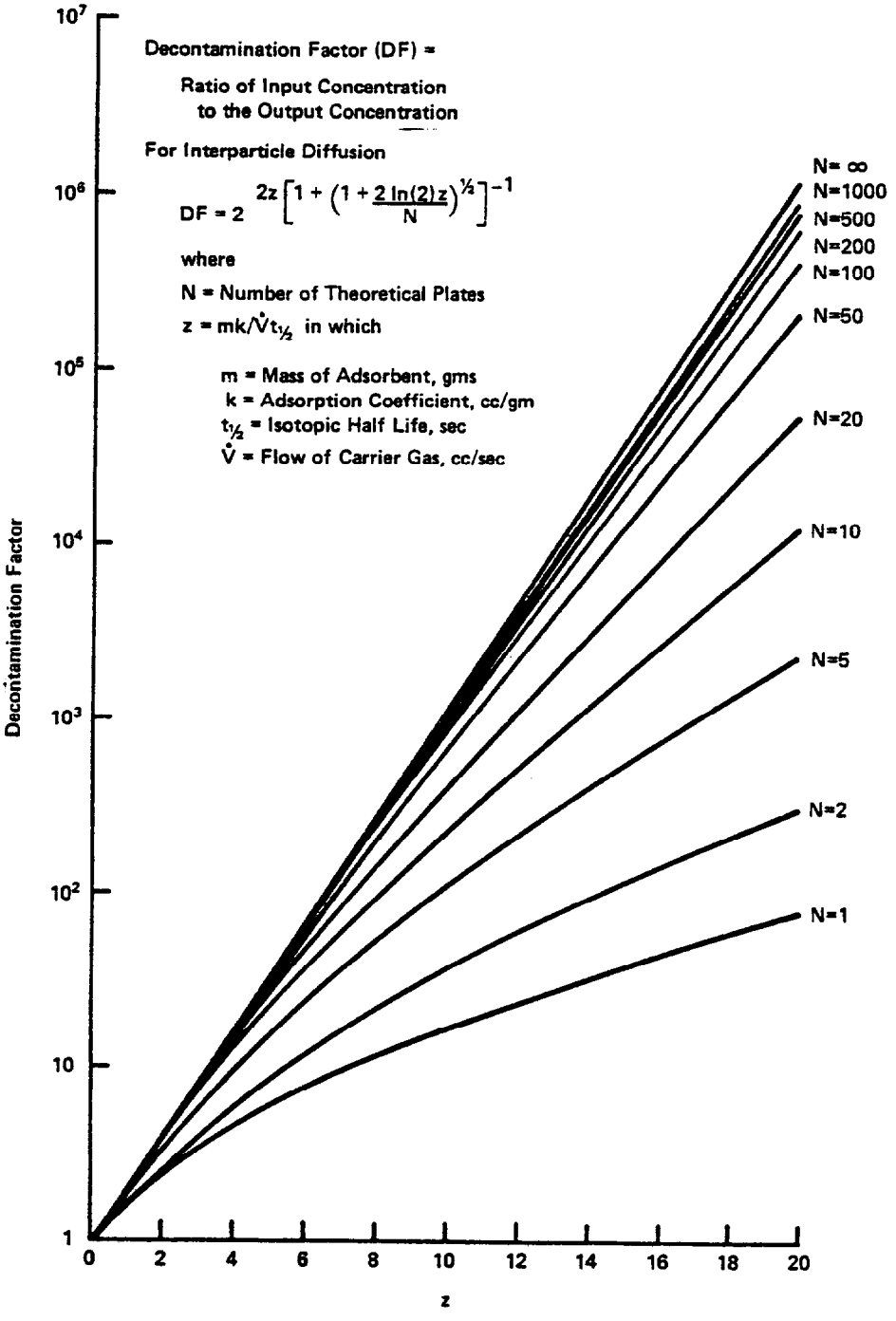

Figure 8 Effect of Interparticle Diffusion on the Decontamination Factor

DISCUSSION

RUTHVEN: I would just like to ask you about the units of your adsorption coefficient. It seems to me there should be a pressure in the denominator there. The units should be milliliters at STP per gram per atmosphere, as far as I can see, because this analysis is based on Henry's Law, and the dimensions must be concentration divided by pressure. Is that not right?

UNDERHILL: Under most conditions, pressure is not a variable, and one should not include more variables than necessary.

RUTHVEN: It's not numerically necessary, but it will be dimensionally incorrect if you do not do it.

UNDERHILL: That is not correct. The bulk adsorption coefficient, k, can be perfectly well defined as

$$k = \frac{\varepsilon + (1 - \varepsilon)\ P}{\rho}$$

where: ε = fractional interparticle void volume, dimensionless.
P = partition coefficient for noble gas between equal volumes of mobile and stationary phase, dimensionless.
ρ = bulk density of the adsorbent, gms/cc.

By this definition, k has units of cc/gm.

RUTHVEN: Yes, but there must be a pressure in there. You can express an adsorption coefficient as a dimensionless quantity, or a ratio of concentrations, but there must be some unit of concentration in the denominator.

UNDERHILL: In this paper, I kept it as being the retention volume divided by the mass of charcoal.

RUTHVEN: But then you are presupposing that you are working always at one atmosphere.

UNDERHILL: Yes. Then in the chapters where I did change the pressure, I had to do some juggling.

RUTHVEN: But it is much more sensible, surely, to go back to basic thermodynamics and use the Henry's Law constant. Then it takes care of pressure dependence. Can I also follow the point up concerning the temperature dependence. I was slightly surprised to see you using the semi-empirical Antoine equation. I would have thought it would have been more normal to use van't Hoff's equation, which will give similar results but has the advantage that the parameters have a clear thermodynamic significance.

UNDERHILL: Over the last century, engineers and chemists have found Antoine's correlation to be both simple and accurate. The available data are not suited to a more complex analysis which would have to include the partitioning of both carrier gas and noble gas between its mobile and stationary phases.

PENBERTHY: Let us get on to one of the basic questions that involves your paper. You alluded to the variability of charcoal. How much control did you exercise over that, and by what laboratory methods did you assess the charcoal?

UNDERHILL: A major part of this paper was to establish the variability of commercially available charcoals as adsorbents of krypton and xenon.

PENBERTHY: What kind of charcoal were you using? How did you make your tests?

UNDERHILL: This was a literature review of charcoals from various reports--some from the Soviet Union, some from West Germany, some from Japan, some from this country.

PENBERTHY: That makes all the things you have presented very uncertain, then. What is this charcoal and what is that charcoal?

UNDERHILL: Once engineers are made aware of the variability of commercial charcoals, they should be able to take this factor into account and design safer systems.

NOBLE GAS SEPARATION FROM NUCLEAR REACTOR EFFLUENTS USING SELECTIVE ADSORPTION WITH INORGANIC ADSORBENTS

D.T. Pence and W.J. Paplawsky
Science Applications, Inc.
4030 Sorrento Valley Boulevard
San Diego, California 92121

Abstract

A radioactive waste gas treatment system utilizing selective adsorption on inorganic adsorbents is described for application to PWRs. The system operates at near ambient pressure, does not require a hydrogen recombiner, has low radioactive gas inventories, and is cost competitive with existing treatment systems. The proposed technique is also applicable for recovery of noble gases from the containment building of a nuclear reactor after an accident. A system design for this application is also presented.

1. Introduction

An integrated off-gas treatment design for nuclear fuels reprocessing was proposed at the 15th Nuclear Air Cleaning Conference[1] that utilizied noble gas separation with selective adsorption on inorganic adsorbents. The noble gas separation portion of the design was demonstrated with an engineering-scale system, and the results of the demonstration reported.[2]

Based on the results of the demonstration tests and subsequent studies and tests, designs for application of the technique for the treatment of nuclear reactor radioactive waste gas streams and nuclear reactor emergency noble gas recovery have been developed and evaluated. The theory, design concepts, and advantages of applying the selective adsorption technique for noble gas separation are discussed.

2. Adsorption Theory

2.1 Dynamic Adsorption

The adsorbents used to separate the noble gases are inorganic synthetic zeolites. These materials are highly crystalline sodium alumino silicates whose adsorptive properties can be modified by replacing the exchangeable cation, sodium, with other cations. The adsorption theory that describes the adsorption behavior of noble gases on zeolites is essentially the same as that used in describing the adsorption behavior of noble gases on activated charocal. In both cases, the adsorption phenomena is based on physical adsorption, rather than chemisorption, and no permanent chemical bond is formed.

Two approaches have been taken to describe the adsorption behavior of the noble gases on activated charcoal: one involving a series of theoretical adsorption chambers[3] and the other is based on the diffusion model concept.[4] Both lead to the conclusion that the predicted breakthrough curves converge to an integral Gaussian distribution equation. The theory most easily described is that based on a series of theoretical chambers or plates. The results of the theory show that the mean residence time of the adsorbate gas in an adsorbent bed is given by

$$t_m = \left(\frac{N - 1}{N}\right) \frac{k_d M}{F} \qquad (1)$$

where t_m = Mean residence time (min)
N = Number of theoretical chambers
k_d = Dynamic adsorption coefficient (cm^3/g)
M = Mass of the adsorbent (g)
F = Flow rate of the gas containing the adsorbent (cm^3/min)

When the number of theoretical plates is large, Equation (1) reduces to

$$t_m = \frac{k_d M}{F} \qquad (2)$$

which is the working equation used for estimating the breakthrough times for noble gases on activated charcoal and also applies to zeolites.

Equation (2) implies that the breakthrough time is independent of: (1) adsorbate concentration, (2) gas mass velocity, and (3) adsorbent particle size. These implications are not completely true. The equation is not valid when the adsorption capacity of the adsorbent is exceeded, which can happen in the concentration of gases using the selective adsorption technique, but is not generally a problem in charcoal delay lines used for noble gases because these operate under conditions in which the noble gas concentrations are well below the adsorption capacity of the charcoal.

The use of the diffusion model can best describe the adsorption limitations with regard to gas velocity and adsorbent particle size. Four basic mass transfer mechanisms are involved in the adsorption of noble gases on adsorbents:[5] (1) longitudinal diffusion in the mobile phase (the tortuosity factor), (2) axial diffusion (eddy diffusion), (3) stationary mass transfer resistance, and (4) mobile phase mass transfer resistance. Mobile phase mass transfer resistance is minor compared with the other mechanisms and is generally ignored.

In deep adsorption beds, the sum of the controlling diffusion variables can be described by a reduced form of the Van Deempter Equation:

$$h = \frac{2\gamma}{v_i} + 2\lambda + C_i v_i \qquad (3)$$

where h = reduced height of a theoretical plate
γ = tortuosity factor for diffusion in the mobile phase
λ = coefficient for axial dispersion
C_i = coefficent for stationary phase mass transfer resistance

v_i = reduced mobile phase velocity

The reduced height of a theoretical plate h is related to the measured height equivalent of a theoretical plate H by the adsorbent particle diameter d_p by

$$H = hd_p \quad (4)$$

and, the height equivalent to a theoretical plate is related to the length of the adsorbent bed L by

$$L = HN \quad (5)$$

where N is the number of height equivalents to a theoretical bed and is approximately equivalent to the number of theoretical chambers described in Equation (1).

The greater the number of height equivalents to a theoretical plate in an adsorbent bed, the sharper will be the breakthrough curve of the adsorbate and the closer to a true Gaussian distribution. Based on a number of studies on the adsorption of noble gases on charcoal,[4-6] it has been determined that the dominant mass transfer mechanisms are: (1) longitudinal diffusion in the mobile phase at low superficial gas velocities, below about 0.3 cm/s (0.6 ft/min); (2) axial diffusion in the intermediate superficial velocity range near 0.3 cm/s; and (3) stationary phase mass transfer at superficial velocities greater than 0.3 cm/s (0.6 ft/min). The smallest value of H which was observed at a superficial velocity of about 0.3 cm/s (0.6 ft/min) was determined to be about 0.9 cm.

Similar results with regard to the controlling mass transfer mechanism were observed in the adsorption of noble gases on zeolites as with activated charcoal. A minimum H value of about 0.5 cm was determined to occur at about 0.6 cm/s (1.13 ft/min). Increasing the superficial face velocity from about 0.6 cm/s to 7.6 cm/s (15 ft/min) increases H to about 1.5 cm.

Therefore, the mean breakthrough time is not independent of gas velocity or adsorbent particle size, but may appear to be so at sufficiently small adsorbent particle sizes and gas velocities.

2.2 Attainable Separation Factors

The adsorption models are defined to apply to deep adsorbent beds but are not clear on what constitutes a deep adsorbent bed. The deviation from a Gaussian distribution can be estimated, but how this can be related to the adsorbent bed diameter, length, the height equivalent to theoretical plate, and the adsorbent bed operating conditions is not well defined. Outside of the nuclear industry, there are few applications that require such high separation factors, so there are few examples to draw from.

In the engineering scale tests using 5-cm (2-in.) diameter columns which varied in length from 1 to 1.7 m (3 to 5 ft), separation factors or decontamination factors (DFs) of greater than 4×10^3 for xenon from air-krypton mixtures were obtained starting with initial concentrations of 2000 ppm of xenon and 200 ppm of krypton. Separation factors greater than 4×10^2 were obtained for krypton in nitrogen. In both cases, the accuracy of the measured DFs were limited by the detection sensitivity of the instrumentation used, and greater DFs were probably attained.

When large-diameter adsorbent beds are used, especially where the length to diameter ratios (L/Ds) are less than about five, appreciable tailing of the adsorbate breakthrough curves can be expected. For this reason, about 50% excess adsorbent was included in the designs presented for an added margin of safety. The smaller the L/D ratio, the smaller will be the adsorbent bed pressure drop for a given flow of gas, so there is considerable incentive to keep the L/D ratio as low as practicable.

2.3 Attainable Concentration Factors

The attainable concentration factors are dependent on the adsorbents' capacities for the particular adsorbate and the dynamic adsorption coefficients, both at the adsorption temperatures and the desorption temperatures. The dynamic adsorption coefficients for krypton and xenon on activated charcoal and several zeolites are shown in Table 1 at various temperatures. Generally, the greater the dynamic adsorption coefficient, the greater will be the attainable DFs. However, to obtain a high concentration factor, the dynamic adsorption coefficient must be small at the desorption temperature as the breakthrough time calculated using Equation (2) still applies. To obtain the desired separation factor between two gases in a gas mixture, an adsorption temperature should be selected that will adequately retain the desired adsorbate while allowing the other to pass through the bed with minimal coadsorption. For example, xenon can be readily separated from krypton using the AX adsorbent. The dynamic adsorption coefficient for xenon on adsorbent AX is about 77 times greater than that for krypton at 25°C. Thus, an appreciable quantity of xenon can be collected on the adsorbent, and the co-adsorbed krypton can be stripped from the adsorbent bed with a reasonably short forward purge of krypton-free air before the xenon breaks through, thereby effecting the xenon-krypton separation.

Adsorbent AK is particularly suitable for krypton removal because of its small adsorption-desorption range, although it does not have the greatest dynamic adsorption coefficient at the preferred adsorption temperature, -80°C. Reasonably high concentration factors can be obtained by desorbing the krypton from this adsorbent at 60°C, keeping the adsorption-desorption temperature range to 140°C.

In addition to ensuring that all of the adsorbate is purged from the adsorbent based on Equation (2), sufficient desorption purge flow should be applied to ensure that the desorbed gas is adequately swept from the bed. For an empty vessel, the relationship of the purge gas versus contaminant gas concentration is given by:

$$V_p = V_v \ln \frac{C_o}{C} \qquad (6)$$

where V_p = purge gas volume

V_v = vessel volume

C_o = initial contaminant concentration

C = final contaminant gas concentration

Because the interparticle void in the bed is less than 0.5, the application of Equation (6) to determine the purge volume represents a conservative estimate.

TABLE 1.

DYNAMIC ADSORPTION COEFFICIENTS OF VARIOUS ADSORBENTS FOR KRYPTON AND XENON

ADSORBENT	DYNAMIC ADSORPTION COEFFICIENT AT VARIOUS TEMPERATURES[a] (°C)							
	-80	-40	0	25	60	100	200	250
KRYPTON								
ACTIVATED CHARCOAL	1,000	240	78	50	27	15	(6)	(4.1)
AK	450	117	52	25	9.0	4.8	1.3	1.1
AX	620	280	123	62	26	11.9	3	1.5
XENON								
ACTIVATED CHARCOAL	60,000	11,000	1,700	720	300	118	(22)	(12)
AK	(>10,000)	(3,800)	480	170	52	18	2.7	1.4
AX	(>50,000)	(>10,000)	7,400	4,800	2,500	1,020	36	1.7

[a]( ) NUMBERS IN PARENTHESES REPRESENT ESTIMATES

3. Proposed System Designs

3.1 PWR Waste Gas Treatment System

3.1.1 Adsorption

A proposed reactor waste gas treatment system flow sheet is given in Figure 1. The gases to be treated are collected from the various sources through a main header which discharges to a surge tank in a manner similar to existing PWR waste gas treatment systems. The gas stream is then passed through a cooler condenser and a particulate filter. Bulk water is removed with a commercial refrigerated dehumidifier that lowers the gas stream dew point to about 2°C. Iodine is removed with a bed of impregnated charcoal or silver-exchanged zeolite.

The remaining water and any carbon dioxide that may be present are removed to about 1 part-per-million in a column filled with Type 4A molecular sieve zeolite. This adsorbent will co-adsorb water and carbon dioxide without retaining appreciable amounts of noble gas or hydrogen. Two adsorbent beds or columns are used in parallel so that one is on service while the other is being regenerated. Adsorption of water and carbon dioxide, if present, is performed near ambient temperature, and the adsorption cycle is about 12 h in duration. Prior to regeneration, the spent adsorbent is given a forward purge of nitrogen for a few minutes to rid any residual noble gas that may be trapped in the interparticle void space. The noble gases are then separated from the hydrogen-nitrogen mixture in a column filled with Type KA adsorbent cooled to -80°C. The feed gas is chilled to -80°C prior to entering the adsorbent columns which have been precooled to -80°C. In this case, krypton and xenon are adsorbed in the adsorbent column while the hydrogen and most of the nitrogen pass through and are discharged to the stack. The cooled, purified gas passes through a heat exchanger to precool the column feed gas prior to passing through the main blower. Eight-hour adsorption cycles are used in a three-column arrangement, so one column can be on service while the other two are in various stages of regeneration or standby.

The desorbed noble gases released during column regeneration are concentrated by a factor of 30 to 40 compared to its initial concentration and are completely free of hydrogen. The desorbed gas is cooled, again to -80°C prior to entering the precooled noble gas concentration columns, where krypton and xenon gases are adsorbed and concentrated again on Type AK adsorbent. The carrier gas is nitrogen and is recycled through a particulate filter, a heat exchanger, a precooler, a recycle pump, the regeneration heater and in a reverse direction through the noble gas removal column prior to passing back through the precooler, cooler, and noble gas concentration column. Hence the noble gas column regeneration cycle is equal to the noble gas concentration column adsorption cycle which is about 120 min in duration. Two noble gas concentration columns are used, so that one can be on service while the other is being regenerated. The collected krypton and xenon are removed from the noble gas concentration columns by a heated stream of nitrogen. During the adsorption-desorption cycle, the noble gases are concentrated again by a factor of about 30 to 40. Because the noble gas concentration columns are heated to about 220°C prior to desorption, the desorption purge times are quite short, about 10-15 min each cycle.

Delay of the radiokrypton and radioxenon is accomplished with a delay line filled with Type AX adsorbent. The gas desorbed from the noble gas concentration

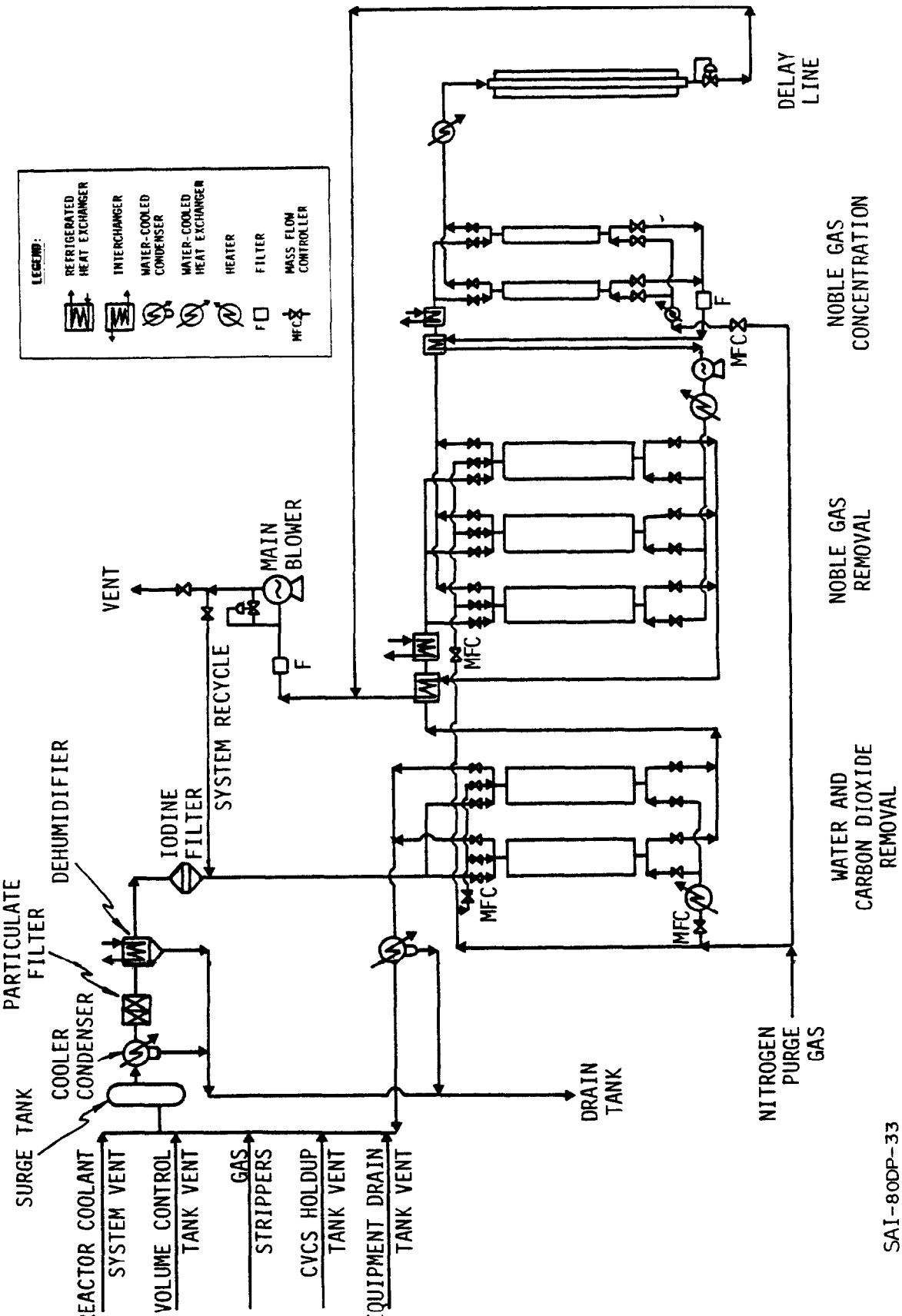

Figure 1. PWR Waste Gas Treatment System Using Selective Adsorption

columns is first cooled to near ambient temperature prior to being discharged to the delay line. Because the desorption flow is only 30 to 45 minutes per day, the delay line does not have to be very large. The delay line is water-jacketed with a closed recirculating system, partially to remove the decay heat and partially for shielding. Effluent from the delay line is discharged to the main blower.

3.1.2 Desorption

Heat up, desorption, and cool down are accomplished with an arrangement that involves an internal recycle system, not shown in Figure 1, so that desorption is not started until the adsorbent bed reaches the desired desorption temperature, thereby limiting the amount of desorption purge gas. Cool down is also accomplished with an internal recirculating system. Provisions are made for complete redundancy of the heaters, recirculating blowers, and heat exchangers by using interconnected parallel circuits. A similar arrangement is provided for the three-column noble gas separation step.

3.2 System Physical and Operating Characteristics

The system characteristics for a PWR Waste Gas Treatment System with a system capacity of 17 m^3/h (10 ft^3/min) are summarized in Table 2. The column dimensions; number of columns; adsorption, purge, desorption characteristics; and heat-up, cool-down, and standby-cycle times are given for the various separation steps. Each of the adsorption steps is accomplished slightly below atmospheric pressure. The column pressure increases to a maximum of about 25 kPa (4 psi) during heat-up for desorption with some of the columns. The driving force for moving the gas through the water and carbon dioxide removal columns and noble gas removal columns during the adsorption cycle is the main blower.

All of the valves are air-operated and sequenced through a programmable microprocessor controller that can readily be adjusted to accommodate changes in throuput rates. Gas and column cooling are accomplished by ethylene glycol and halocarbon refrigeration systems.

3.3 Expected Operating Performance

The expected decontamination factors for krypton and xenon in the noble gas removal columns are greater than 4×10^2 for krypton and 4×10^3 for xenon. The described delay line will provide a hold-up time of about 3 d for krypton and about 90 d for xenon.

3.4 Other Design Considerations

3.4.1 Operation With Hydrogen Gas Mixtures

The described system does not require a hydrogen recombiner as krypton and xenon are separated from the hydrogen-nitrogen mixture prior to concentration and delay for decay. Even if some oxygen were introduced into the system, the probability of a hydrogen conflagration or detonation would be very small as there are no heat or spark sources during adsorption. All of the valves are fluorocarbon-seated ball or plug valves. In addition, the hydrogen-gas mixture is maintained below ambient temperature until discharge through the main blower. Air dilution of the gas stream may be desirable before entering the main blower.

TABLE 2.
PWR WASTE GAS TREATMENT SYSTEM CHARACTERISTICS

	WATER/CARBON DIOXIDE REMOVAL	NOBLE GAS REMOVAL	NOBLE GAS CONCENTRATION	DELAY LINE
COLUMN DIMENSIONS (DIAM IN IN. X LENGTH IN FT.)	8 x 2.5	20 x 10	8 x 4.5	2 x 30
NUMBER OF COLUMNS	2	3	2	1
MASS OF ADSORBENT/ COLUMN (LBS)	50	900	77	36
ADSORPTION				
TIME (MIN)	720	480	120	30/DAY
FLOW RATE (FT^3/MIN)	10	10	3	0.2[a]
FORWARD PURGE				
TIME (MIN)	5	10	-	-
FLOW RATE (FT^3/MIN)	3	10	-	-
DESORPTION				
TIME (MIN)	30	120	10	-
TEMPERATURE (°C)	220	100	250	-
FLOW RATE (FT^3/MIN)	2	3	0.2	-
HEAT-UP CYCLE TIME (MIN)	120	180	120	-
COOL-DOWN CYCLE TIME (MIN)	180	300	200	-
STANDBY TIME	385	350	150	-

[a] INTERMITTENT

3.4.2 System Capacity

System capacity requirements vary considerably depending on the reactor design. The selected 17 m^3/h (10 ft^3/min) system design would probably accommodate two 1000 MWe PWRs, depending on the letdown rates, gas stripping rates, and venting arrangements. The system is insensitive to extreme variations in noble gas concentrations and very flexible for varying throughput rates. The system is expected to operate satisfactorily with varying feed-gas rates from less than one-tenth of its rated capacity to twice the rate capacity. If the increased throughput rate is maintained for more than a few hours, krypton will eventually break through the noble gas removal columns unless the noble gas removal column cycle times are adjusted through the microprocessor control system to reduce the standby cycle times.

At very low throughput rates, it may be desirable to add nitrogen to the feed stream. The capability for nitrogen addition to the feed gas would be particularly attractive if appreciable oxygen in-leakage were detected.

3.4.3 Krypton Recovery

If it were considered desirable, krypton could easily be recovered with this system by adding two more columns containing Type AZ adsorbent between the noble gas removal and the noble gas concentration columns. Xenon would be separated from krypton on these columns and desorbed to the delay line. The noble gas concentration columns would then serve as krypton removal and concentration columns. The krypton desorbed from these columns would be collected with a freeze trap and transferred to storage cylinders.

3.5 System Cost

The estimated cost of the described system shop-fabricated, skid-mounted, and complete with instrumentation is $1,400,000. The power requirements are estimated to be about 25 Kw for full-capacity operation.

3.6 Application to BWRs

The described waste gas treatment system would certainly be applicable for BWR off-gas treatment downstream of the BWR recombiners. The system capacity would have to be somewhat larger to accommodate the larger condenser in-leakage rates. The oxygen would be separated from the krypton and xenon in the noble gas removal columns.

Whether or not the system would operate safely without recombiners would have to be determined in a more comprehensive safety analysis than has been considered at this point.

3.7 Advantages of the Proposed Design

The advantages of the proposed system design as compared with presently used control techniques are:

(1) Nonpressurized system. Because the proposed system operates near ambient pressure, there is considerably less probability for an accidental release of the recovered radioactive noble gases.

(2) System inventories are low. With the exception of the delay line, the maximum noble gas inventory in any part of the system is only that accumulated in 8 hours of operation. Even with a complete power failure, the radioactive release from the delay line would be insignificant.

(3) Lower space requirements. The process equipment can be installed in a very compact arrangement. All but the noble gas columns are quite small. Because the radioactive gas inventories are quite small, less isolation and shielding is required.

(4) No external dilution steam is required. Because hydrogen recombiners are not required for the PWR system, no external dilution steam or large nitrogen recycle gas stream is needed.

(5) Cost competitive. The installed capital and operating costs of the proposed system are estimated to be less than presently used systems.

4. Emergency Noble Gas Recovery System

4.1 General

Since the Three Mile Island Unit 2 accident, there has been considerable interest in emergency nuclear reactor noble gas recovery systems. A flow diagram showing how such a system, using selective adsorption, could be applied is shown in Figure 2. The proposed system involves particulate, iodine, and water and carbon dioxide removal as pretreatment steps prior to the noble gas separation and recovery steps. A more detailed system design is presented in Figure 3. The process operations are similar to that described for the PWR waste gas treatment system to the noble gas separation columns, except the components are considerably larger.

4.2 Noble Gas Recovery

Oxygen and hydrogen are separated from krypton and xenon in the noble gas separation columns and are discharged through the main blower. The desorbed krypton and xenon are cooled to ambient temperature and passed through a column of Type XA adsorbent, where the xenon is retained and krypton passes through.

Xenon is desorbed from the xenon removal columns at a desorption temperature of about 250°C, then cooled and compressed for tank storage. A delay line could be used; but because of the large volume of xenon that could conceivably be released during a major accident at a 1000 MWe unit, nearly 1900 ft^3, compressed storage appears to be more cost effective.

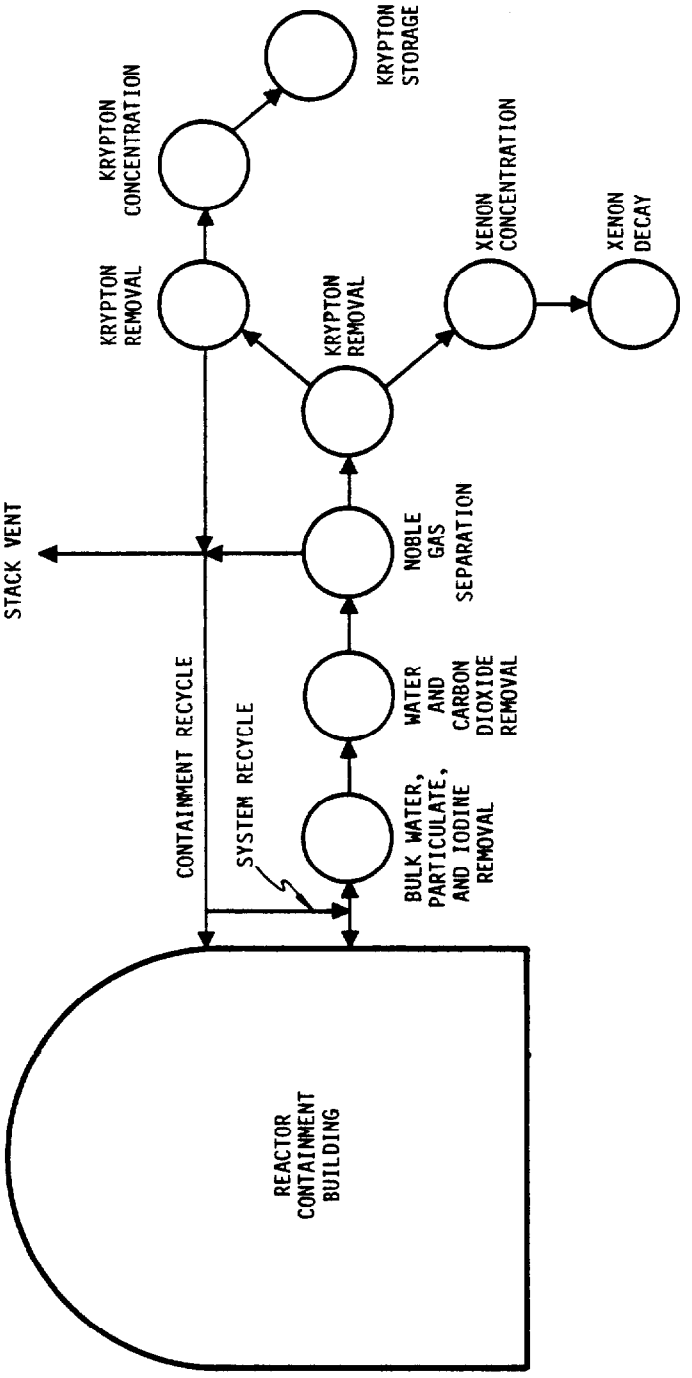

Figure 2. Emergency Noble Gas Recovery System Using Selective Adsorption

SAI-80DP-31

Figure 3.
Emergency Noble Gas Recovery System
for Reactor Containment Building

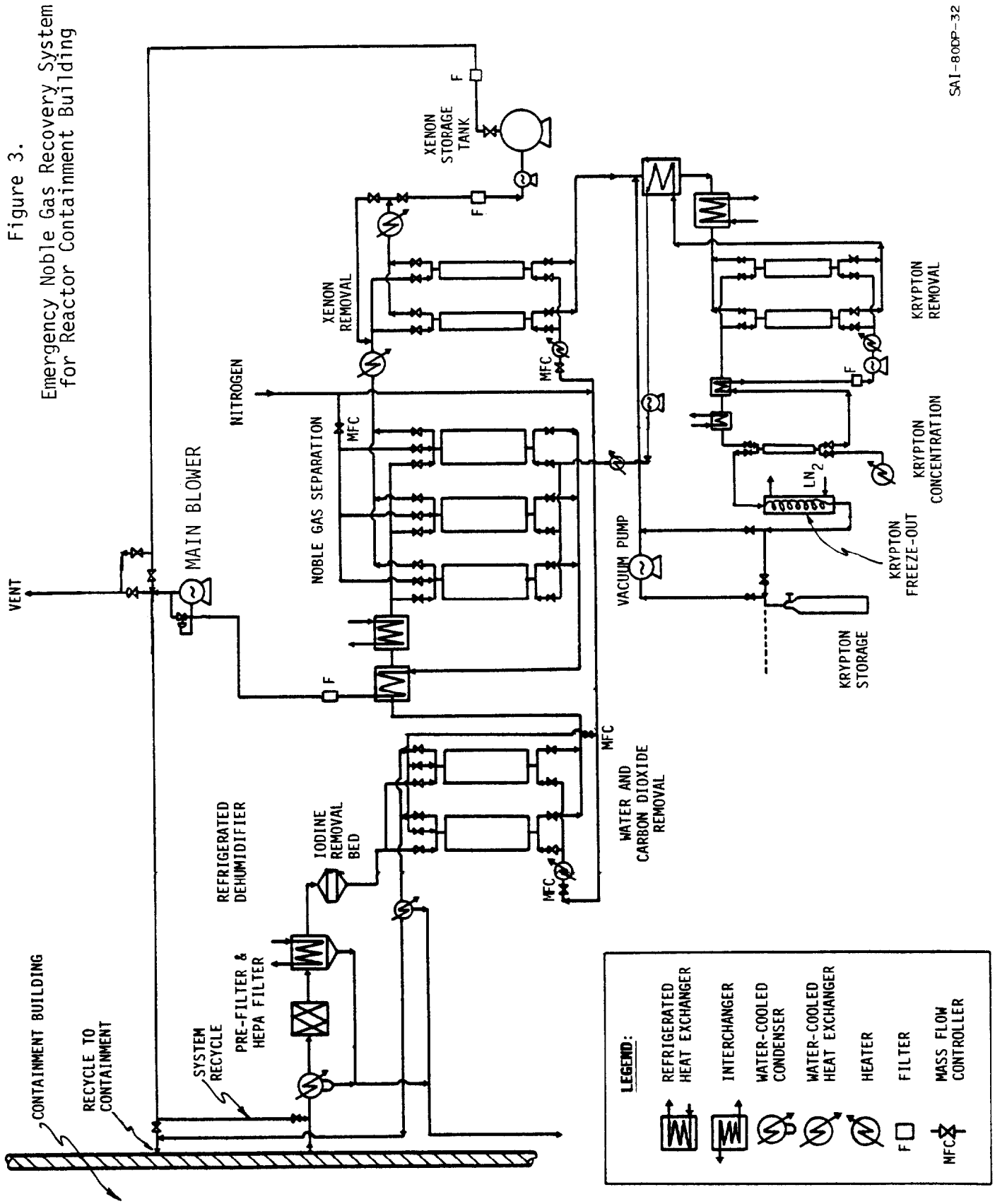

The krypton and nitrogen gas mixture that passes through the xenon removal columns is cooled to -80°C, and the krypton adsorbed in a column filled with Type AX adsorbent that has been cooled to -80°C. The krypton is desorbed at 60°C, cooled again to -80°C and concentrated further by adsorption on a krypton concentration column filled with the same adsorbent with a closed recirculating stream of nitrogen gas. The krypton concentration column is also desorbed at 60°C, and the desorbed krypton is collected on a liquid nitrogen-cooled freeze-out trap. The collected krypton is then warmed and expanded to the krypton storage cylinders. Residual krypton in the freeze-out trap and filling lines is removed with a vacuum pump and recycled to the krypton removal column feed. The krypton concentration in the storage cylinders will be greater than 90%. This technique has been demonstrated in the engineering-scale tests.

4.3 System Characteristics

The proposed nuclear reactor emergency noble gas recovery system characteristics for a 340-m^3/h (200-ft^3/min) capacity system are summarized in Table 3. The expected system performance for the proposed design is DFs of greater than 10^2 for krypton and greater than 10^3 for xenon.

The entire system could be skid-mounted for quick transportation, installation, and hookup. Column and heat-exchanger cooling could be done with either liquid nitrogen or with refrigeration systems. The estimated cost for a shop-fabricated, skid-mounted system is about $6,000,000, including the refrigeration equipment.

Even through the oxygen concentration would probably be near ambient levels in the system feed gas, the need for hydrogen recombiners for gas pretreatment for the proposed system appears unnecessary.

If post-accident noble gas recovery systems are considered necessary, the proposed design, using selective adsorption, appears to be the most cost-effective approach.

5. Conclusions

The use of selective adsorption with certain inorganic adsorbents for the separation and concentration of noble gases shows considerable promise for a number of applications in the nuclear industry. This technique offers some significant safety and cost advantages compared with other techniques. The technique utilizes existing technology and no new components need to be developed. Although the technique has been demonstrated with an engineering-scale system, pilot-plant demonstration with extended operation needs to be performed before it can be considered for full-scale design and application.

TABLE 3. EMERGENCY NOBLE GAS RECOVERY SYSTEM CHARACTERISTICS

	WATER/CARBON DIOXIDE REMOVAL	NOBLE GAS REMOVAL	XENON REMOVAL	XENON RECOVERY	KRYPTON REMOVAL	KRYPTON CONCENTRATION	KRYPTON FREEZE-OUT
COLUMN DIMENSIONS (DIAM IN IN. X LENGTH IN FT)	20 x 4.5	72 x 12	18 x 6.5	-	24 x 6	3 x 2	(0.2 FT^3)
NUMBER OF COLUMNS	2	3	2	2 TANKS	2	1	1
MASS OF ADSORBENT/ COLUMN (LBS)	400	14,700	500	30 FT^3/ TANK	850	10	-
ADSORPTION							
TIME (MIN)	720	480	90	60	90	60	30
FLOW RATE (FT^3/MIN)	200	200	50	~ 2	50	3	0.05
FORWARD PURGE							
TIME (MIN)	20	10	5	-	-	-	-
FLOW RATE (FT^3/MIN)	20	20	15	-	-	-	-
DESORPTION							
TIME (MIN)	30	90	60	-	60	30	3
TEMPERATURE (°C)	220	100	250	-	60	60	25
FLOW RATE (FT^3/MIN)	10	50	2	-	3	0.05	-
HEAT-UP CYCLE TIME (MIN)	120	180	120	-	120	60	60
COOL-DOWN CYCLE TIME (MIN)	300	360	180	-	200	60	60
STANDBY TIME (MIN)	250	320	115	420	100	270	327

6. References

1. D.T. Pence, C.C. Chou, J.D. Christian, and W.J. Paplawsky, "Noble Gas Separation with the Use of Inorganic Adsorbents", Proceedings 15th DOE Nuclear Air Cleaning Conference, CONF-78091, p. 512 (August 1978).

2. D.T. Pence, C.C. Chou, and W.J. Paplawsky, An Integrated Off-Gas Treatment System Design for Nuclear Fuel Reprocessing Plants Using Selective Adsorption, SAI/00979-2 (August 1979).

3. D.P. Siegwarth, C.K. Neulander, R.T. Pao, and M. Siegler, "Measurement of Dynamic Adsorption Coefficients for Noble Gases on Activated Carbon", Proceedings 12th AEC Air Cleaning Conference, CONF 720 823, p. 28 (August 1972).

4. D.W. Underhill, Dynamic Adsorption of Fission-Product Noble Gases on Activated Charcoal, NYO-841-8 (April 1967).

5. G. Collard, M. Put, J. Boothaerts, and W.R.A. Goossens, "The Delay of Xenon on Charcoal Beds", Proceedings of the 14th ERDA Air Cleaning Conference, CONF-760822, p. 947 (August 1976).

6. K.P. Strong and D.M. Levins, "Dynamic Adsorption of Radon on Activated Charcoal", Proceedings 15th Nuclear Air Cleaning Conference, CONF-780819, p. 627 (August 1978).

DISCUSSION

ABRAMS: Have you done any analysis of what a system like that would cost for a pressurized water reactor?

PENCE: For this particular system, based on a rough analysis but not just out of the air, it would cost about $1.4 million. This is for a shop-fabricated uninstalled ten cubic foot per minute system.

ABRAMS: Is there much change if the flow rate goes down to 2 to 4 cfm?

PENCE: No. That is one advantage of the system I did not mention. It can operate at essentially any concentration and over a wide range of fluctuating flow rates. You preset the adsorption cycle (unless you know it is going to remain low), and then you can adjust it. The valves are all operated on a programmable system and you can adjust it even while in process.

REMOVAL OF Kr FROM N_2 BY SELECTIVE ADSORPTION*

D.M. Ruthven, J.S. Devgun and F.H. Tezel
Department of Chemical Engineering
University of New Brunswick
Fredericton, N.B., Canada

T.S. Sridhar
Atomic Energy of Canada Limited
Whiteshell Nuclear Research Establishment
Pinawa, Manitoba, Canada ROE 1LO

To be presented at 16th DOE Nuclear Air Cleaning Conference, San Diego, California, October 20 - 23rd 1980.

Abstract

The results of a chromatographic study of the sorption kinetics and equilibria for N_2 and Kr on several zeolitic adsorbents are presented. Of the adsorbents investigated the most promising for selective removal of Kr from the off-gas of nuclear fuel processing facilities is H-mordenite. It is shown that the selectivity of this adsorbent towards Kr may be increased by de-alumination and at low temperatures the selectivity of the de-aluminated mordenite becomes comparable with that of the best activated carbon adsorbents.

Introduction

During the fission of ^{235}U fuels several different isotopes of the noble gases Kr and Xe are formed. These gases are retained within the fuel rod and released when the fuel rod is dissolved during reprocessing. Most of the Kr and Xe isotopes are either stable species or else decay rapidly to stable species. The two longest lived isotopes are ^{133}Xe (half-life 5.3 days) and ^{85}Kr (half-life 10.7 years). The half-life of ^{133}Xe is sufficiently short that, provided the irradiated fuel is stored for a period of several months prior to reprocessing, it will decay to an insignificant level. Although it is formed only in relatively small amounts, the ^{85}Kr isotope has significant radioactivity associated with it. Future regulatory standards will probably require that the active krypton be removed from the off-gas of fuel processing facilities prior to venting. The active krypton would then be packaged for storage or permanent disposal.

The problem of separating trace amounts of Kr (and Xe) has attracted much research during the past decade. Several different types of process have been considered and are in various stages of technological development but no single process has yet emerged with a clear advantage. Useful reviews of the state of technology have been given by Keilholtz[1], Slansky[2] and more recently but in less detail by Bendixsen and Knecht[3]. Among the more promising process routes are the following:

*Issued as AECL-7004

1. Cryogenic distillation

2. Selective adsorption (in fluorocarbons, carbon tetrachloride, and liquid carbon dioxide)

3. Diffusion through a permselective membrane

4. Selective adsorption

The Adsorption Process

The present study is restricted to the selective adsorption process. This type of process operates on well established principles and has been successfully applied in the nuclear industry for the removal of Kr and Xe from the He coolant in the High Temperature Gas-cooled Reactor (HTGR)[4,5]. Adsorption systems are at present being developed for the clean-up of off-gases from fuel processing plants[6,7]. The success of the adsorption process depends on the availability of an adsorbent with a sufficiently high selectivity for the component or components which are to be removed.

In reviewing the earlier developments it is important to keep in mind the gas stream composition in the different applications. For example, in the HTGR with He as the coolant, the adsorber system is required to remove traces of Kr and Xe from the He carrier. Also, in the reprocessing of HTGR graphite fuel, the off-gas consists of traces of Kr and Xe in a stream of CO_2[8]. However, the off-gas from reprocessing plants operating on the Purex process, consists of traces of Kr and Xe in a stream of air. Hence the adsorption data for a particular gas obtained for one gaseous system would not be directly applicable to another even on the same sorbent. The choice of the adsorbent and the performance of the process may be profoundly affected by the nature and quantities of other gases present.

It is convenient to subdivide the adsorption processes involving radioactive species into two classes, depending on whether the adsorber bed is used to effect a true separation of the radioactive species or merely to provide a time delay to allow the species to decay to stable isotopes. The separation processes may be further classified according to the nature of the process cycle.

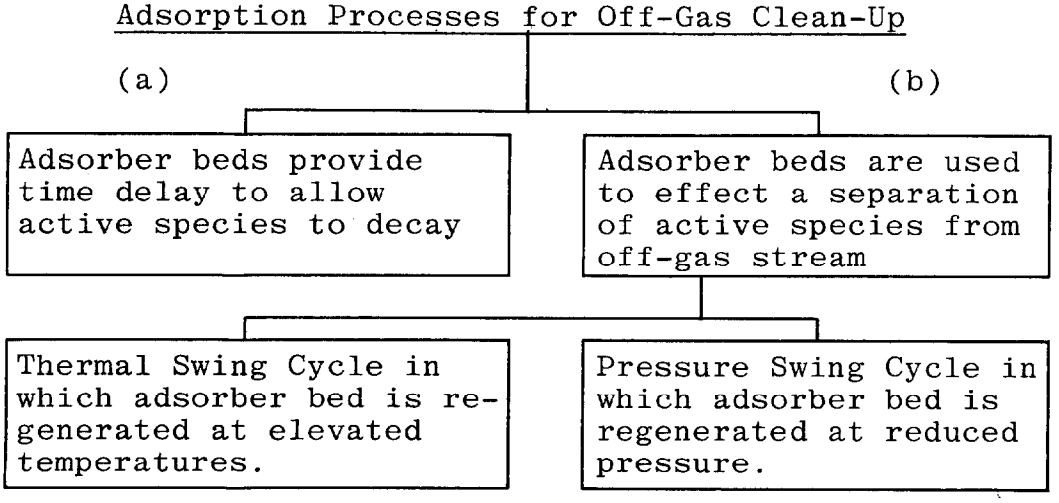

Scheme (a) is the obvious choice for relatively short-lived species like ^{133}Xe, as in the reactor off-gas clean-up systems, but it is impractical for dealing with the longer-lived species such as ^{85}Kr. This scheme was used successfully to remove the short-lived species from the coolant in the Dragon HTGR. A detailed description of the system has been given, including experimental breakthrough curves, dynamic adsorption capacity data and other detailed design information[4]. The system used consisted of large water-cooled beds to provide a minimum delay of 200 hours for Xe and 15 hours for Kr, followed by smaller beds operated at -190°C, cooled by liquid nitrogen, which provided a delay time of 60 days for Xe and 3 days for Kr. The ^{85}Kr isotope, as well as the stable isotopes from the delay beds, were removed by further adsorption beds operating by thermal swing. Activated carbon was used as the adsorbent in all beds.

Although active carbon sorbent has been successfully employed in a plant-scale operation as above for ^{85}Kr removal, such a sorbent has a major drawback in its application to the off-gas clean-up in Purex reprocessing plants. The presence of oxygen in the off-gases of such plants renders the carbon sorbent susceptible to fire hazards.

The adsorption process has the advantages of simplicity, reliability and relatively low operating costs. If an inorganic adsorbent can be found with a selectivity and capacity comparable to activated carbon, then the adsorption process would probably emerge with a clear advantage over other processes. The development of a selective adsorption process using an aluminosilicate adsorbent (a zeolite molecular sieve) has been recently reported[7], but no details of the adsorbent were given. Since the adsorbent is critical to the success of such a process, the search for a suitable adsorbent has been the primary objective of the present research.

Equilibrium and Kinetic Separations

Most of the established selective adsorption separation processes depend on differences in the adsorption equilibrium for the various components of the mixed gas stream. For example, in the Dragon HTGR system referred to above, Kr and Xe are adsorbed more strongly than He on activated carbon so that these gases are selectively removed. Since adsorption is an exothermic process the adsorption equilibrium constant will always increase as the temperature is decreased. This means that both the equilibrium selectivity and capacity will be greater at low temperatures and, for the efficient removal of small traces of undesirable impurities, low-temperature operation is generally required.

In certain cases however selective separation may be based on differences in adsorption rate rather than on differences in adsorption equilibrium and such processes are here referred to as kinetic separations. Well established examples include the carbon molecular sieve Pressure Swing Adsorption air separation process[9] and the Mobil process for separation of C_8 aromatics[10]. An extreme example of a successful kinetic separation is the separation of the straight chain hydrocarbons from branched and cyclic isomers using a 5A molecular sieve. The critical diameter of the branched hydrocarbon is too great to allow penetration of the zeolitic windows even though adsorp-

tion is thermodynamically favourable. In this example the kinetic separation factor approaches infinity but it is only in exceptional cases that such a complete kinetic separation can be achieved.

Choice of Adsorbent - Preliminary Considerations

Because of the high proportion of N_2 present in Purex reprocessing off-gas, it is evident that the main requirement for efficient removal of Kr is a high selectivity for Kr relative to N_2. On most adsorbents O_2 is adsorbed less strongly than N_2 and since the O_2 concentration will always be much lower than the N_2 concentration, competitive adsorption of O_2 is unlikely to present a severe problem. Equilibrium adsorption data (Henry's Law constants) for both Kr and N_2 are available for several adsorbents and some of the values are compared in Table I. Of these adsorbents activated carbon has the highest equilibrium separation factor (α, defined as $(K_p)_{Kr}/(K_p)_{N_2}$) and it is for this reason that activated carbon has been the preferred adsorbent in most Kr removal processes. The important role played by the cation in modifying the equilibrium properties in zeolite sorbents is illustrated by the data of Bosacek for LiX and KX[16].

Table I. Summary of adsorption equilibrium constants for Kr and N_2 on various adsorbents (literature data)

Adsorbent	$(K_p)_{Kr}$ x 100 mL·STP/(g·Pa)	$(K_p)_{N_2}$ x 100 mL·STP/(g·Pa)	α	$(-\Delta H/R)_{Kr}$ K	$(-\Delta H/R)_{N_2}$ K
Activated Carbon	0.11-0.14 (11)	-	-	2650	-
	0.54-0.14 (12)	-	-	2500	-
	0.13 (13)	0.014	9	2800	2265
	0.019 (12)	-	-	1860	-
5A Sieve	0.045 (14)	-	-	2000	-
	0.016 (15)	0.023	0.7	2120	2500
4A Sieve	0.020 (15)	0.014	1.5	2140	2200
LiX Sieve*	0.18 (16)	0.34	0.54	-	-
KX Sieve*	0.42 (16)	0.17	2.5	-	-
H-Chabazite	0.034 (17)	0.009	3.7	2150	2400
Natural (Ca) Chabazite	0.038 (14)	-	-	2500	-
H-Mordenite	0.06 (14)	-	-	2080	-
Na-Mordenite	0.14 (18)	0.06	2.4	2340	3700

* Values of K_p and α are at 273 K except for values with asterisks which refer to 195 K. $(-\Delta H)_{Kr}$ and $(-\Delta H)_{N_2}$ are limiting heats of adsorption.

Among the zeolitic adsorbents for which data are available, H-chabazite has the highest selectivity at 273 K. However the difference between the heats of sorption of N_2 and Kr is smaller for most of the zeolites than for activated carbon. This means that the selectivity cannot be markedly increased by reducing the temperature. For some of the adsorbents the heat of sorption of N_2 is actually higher than that of Kr. In such cases the Kr selectivity can be increased by raising the temperature but only at the expense of a sharp decrease in adsorptive capacity.

Only very limited kinetic data are available for the sorption of N_2 and Kr on zeolitic adsorbents so the possibilities of finding an adsorbent with a sufficiently large difference in adsorption rates to provide an efficient kinetic separation could not be assessed a priori. However, in general, rates of intracrystalline diffusion in molecular sieve adsorbents are more sensitive than the sorption equilibria to small differences in sieve structure or cation content. Although Kr is a somewhat larger molecule than N_2 it is monatomic, and the possibility of finding a molecular sieve adsorbent which adsorbs Kr much more rapidly than N_2 cannot therefore be ruled out. If such an adsorbent were to be found, it could clearly provide a basis for an efficient kinetic separation, and this is the rationale behind the present investigation on zeolite sorbents.

Experimental

The Chromatographic Method

In the chromatographic method, adsorption rates and equilibria are determined by analysis of the response peaks generated when a pulse of adsorbate is injected into an inert carrier stream flowing through a column packed with adsorbent. For adsorbent screening the method offers advantages of speed, cost and flexibility over conventional gravimetric or volumetric methods and the presence of a large excess of carrier gas ensures isothermal operation and minimizes the intrusion of heat transfer resistances[19]. The major disadvantage of the method is the need to eliminate or allow for axial dispersion.

The theory of the chromatographic method has been fully discussed by Haynes et al.[20-22]. Comparative measurements carried out by Shah and Ruthven[23] have confirmed the consistency of both the diffusional time constants and equilibrium isotherms derived from gravimetric and chromatographic studies of the same systems. In order to derive the equilibrium and kinetic parameters, it is necessary to match the experimental response peak to an appropriate mathematical model of the system. The simplest approach is to match the first and second moments of the theoretical and experimental response peaks. According to the model of Haynes and Sarma[22], which includes most of the important effects such as external film mass transfer resistance and macropore diffusional resistance as well as intracrystalline diffusion and axial dispersion, the moments of the response peak are given by:

$$\mu = \frac{L}{v} \left\{ 1 + \left(\frac{1 - \varepsilon}{\varepsilon} \right) K_p \right\} \qquad (1)$$

$$\frac{\sigma^2}{2\mu^2} = \frac{D_L}{vL} + \left(\frac{\varepsilon}{1-\varepsilon}\right)\left(\frac{v}{L}\right)\left\{\frac{R_p}{3k} + \frac{R_p^2}{15\Theta D_p} + \frac{r^2}{15K_p D_c}\right\} \cdot \frac{1}{\left[1 - \frac{1}{\left(\frac{v\mu}{L} - 1\right)^2}\right]} \qquad (2)$$

where the first moment (μ) is defined by:

$$\mu = \frac{\int_0^\infty c.t.dt}{\int_0^\infty c.dt} \qquad (3)$$

and the second moment (σ^2) is defined by:

$$\sigma^2 = \frac{\int_0^\infty (t-\mu)^2 \cdot c \cdot dt}{\int_0^\infty c \cdot dt} \qquad (4)$$

In these expressions c refers to the outlet adsorbate concentration in response to a pulse injection at the column inlet at time zero. For a component which is strongly adsorbed ($K_p >> 1$) eq. (2) reduces to:

$$\frac{\sigma^2}{2\mu^2} = \frac{D_L}{vL} + \left(\frac{\varepsilon}{1-\varepsilon}\right)\left(\frac{v}{L}\right)\left\{\frac{R_p}{3k} + \frac{R_p^2}{15\Theta D_p} + \frac{r^2}{15K_p D_c}\right\} \qquad (5)$$

For a weakly adsorbed species such as He, $\mu \approx L/v$ and $(\sigma^2/2\mu^2) \approx (D_L/vL)$.

Tailing of the response curves becomes pronounced when mass transfer resistance is high and this makes the accurate calculation of the second moments difficult, leading to scatter in the experimental results. Various alternative methods of analysing the uptake curves by matching in the time domain or by matching Laplace or Fourier transforms have been suggested[24-28] in order to avoid this problem. For the initial analysis of our experimental data we have used only the moments analysis which is simple and economical on computing time.

From eqs. (2) and (5) it is evident that the second moment of the chromatographic response peak (or the ratio $(\sigma^2/2\mu^2)$ depends on the extent of axial diffusion in the column as well as on the mass transfer resistance. Further, the mass transfer term (the second term on the right hand side of eq. (5)) contains contributions from film and macropore diffusion resistance as well as from micropore (intracrystalline) diffusion. In order to measure intracrystalline diffusional time constants (D_c/r^2) by the chromatographic method it is therefore

necessary to eliminate or allow for the contributions to the second moment arising from axial diffusion and the extracrystalline mass transfer resistance. The effect of extracrystalline (film and macropore) mass transfer can be reduced to an insignificant level by using small adsorbent particles. Assuming transport within the macropores to occur mainly by molecular diffusion and a Sherwood number of 2.0 (the low Reynolds number limit), equation (5) becomes:

$$\frac{\sigma^2}{2\mu^2}\frac{L}{v} = \frac{D_L}{v^2} + \left(\frac{\varepsilon}{1-\varepsilon}\right)\left\{\left(\frac{1}{3} + \frac{\tau}{15\Theta}\right)\frac{R_p^2}{D_m} + \frac{r^2}{15K_p D_c}\right\} \qquad (6)$$

Typical values of the tortuosity factor (τ) and porosity (Θ) are 3 and 0.3 respectively so, provided that $R_p^2/D_m \ll \sigma^2 L/2\mu^2 v$, the contributions from film and macro resistance will be negligible. Since the particle size and molecular diffusivity are known, the validity of this condition for any particular system is easily checked.

Axial dispersion presents a more serious problem since the correction may be quite significant, particularly at the low gas velocities necessary for laboratory measurements. The axial dispersion coefficient (D_L) depends on the molecular diffusivity, the gas velocity and the particle radius. One of the more widely used correlations is that of Edwards and Richardson[29]:

$$D_L = 0.73\, D_m + \frac{vR_p}{1 + \dfrac{4.85\, D_m}{vR_p}} \qquad (7)$$

Range of validity: $0.019 < R_p < 0.3$ cm

$0.008 < R_e < 50$

Although it has been claimed that this correlation is applicable over a wide range of particle sizes, recent studies[30] have shown that for smaller particles the deviations may be quite severe. These deviations are important only at high gas velocities, and at low gas velocities within the laminar regime the data of most authors conform approximately to the simplified expression:

$$D_L \overset{\sim}{\sim} 0.7\, D_m \qquad (8)$$

which is essentially the form to which eq. (7) reduces for small values of vR_p. However, it has been emphasized[30] that, in experimental studies of mass transfer rates by the chromatographic method, the axial diffusion characteristics of the particular column should first be established directly.

The axial dispersion coefficient may be determined by measuring the chromatographic response for a He pulse in a stream of the more strongly adsorbed component [N_2 or Kr]. Since He is only weakly adsorbed $\sigma^2/2\mu^2 \approx D_L/vL$. Furthermore, D_L depends only on the gas velocity, the molecular diffusivity and the packing of the column. Since the molecular diffusivity for He in N_2 is the same as for N_2 in He it is evident that, for a given column and gas velocity, the dispersion coefficient determined from the He pulse experiment should be the same as for a N_2 pulse in a He carrier. Since the molecular diffusivities of He-Kr and He-N_2 differ by only about 10%, the same dispersion coefficient may be used for the Kr pulse experiments. Once the value of D_L is established the mass transfer resistance may be calculated simply from the difference $\sigma^2L/2\mu^2v - D_L/v^2$. Accurate values can of course be found only when the contribution from axial dispersion is relatively minor in comparison with the mass transfer resistance.

In the low Reynolds number region D_L is approximately independent of gas velocity (eq. (8)) so it may be seen from eq. (6) that a plot of $\sigma^2L/2\mu^2v$ vs. $1/v^2$ should be linear with slope D_L and intercept equal to the mass transfer resistance term. In fact D_L is expected to increase somewhat with gas velocity (eq. (7)) so that a gentle curve rather than a straight line is to be expected in such a plot when the gas velocity is varied over a wide range. It is in principle possible to determine both the axial dispersion coefficient and the mass transfer resistance from the slope and intercept of such a plot. However in practice, because of experimental scatter, it is often difficult to determine the slope accurately and independent measurement of D_L using the He pulse method is therefore preferable.

The maximum intracrystalline diffusivity which can be reliably measured by the chromatographic method is limited by the requirement that extracrystalline mass transfer resistance must be small compared with intracrystalline resistance:

$$15\ K_p\ D_c/r^2 \ll D_m/R_p^2 \qquad (9)$$

This limitation is well known but there is also a less well publicized lower limit which is imposed by the requirement that the chromatographic pulse must establish equilibrium with the intracrystalline adsorbed phase in a time period that is small compared with the retention time in the column. If intracrystalline diffusion is too slow, the adsorption peak will pass through the column without significant adsorption and no information concerning either the adsorption equilibrium or the kinetics can then be obtained. This requirement has been discussed by Habgood and MacDonald[31]. Their criterion can be expressed in two forms:

$$\sigma^2/2\mu^2 < 1/8,\ K_pD_c/r^2 > v/3L \qquad (10)$$

Apparatus and Method

The apparatus is shown schematically in Figure 1. The column is made of stainless steel tube (i.d., 0.63 cm) and four different

lengths (7.62 cm, 10.16 cm, 11.43 cm, 19.4 cm) were used. The column length was selected to give a convenient retention time for the particular adsorbent system under investigation. Measurements were made at several temperatures over a range of gas velocities. A Gow-Mac thermal conductivity detector (model 40-05C), fitted with W2X elements, was used with the appropriate bridge and power supply to monitor the concentration of the gas leaving the adsorption column. A Perkin-Elmer gas-sampling valve fitted with a 1-mL sample loop was used to inject pulses of either N_2 or Kr into the carrier stream at the column inlet. Linearity of the system was confirmed in preliminary experiments with a 5-mL sample loop.

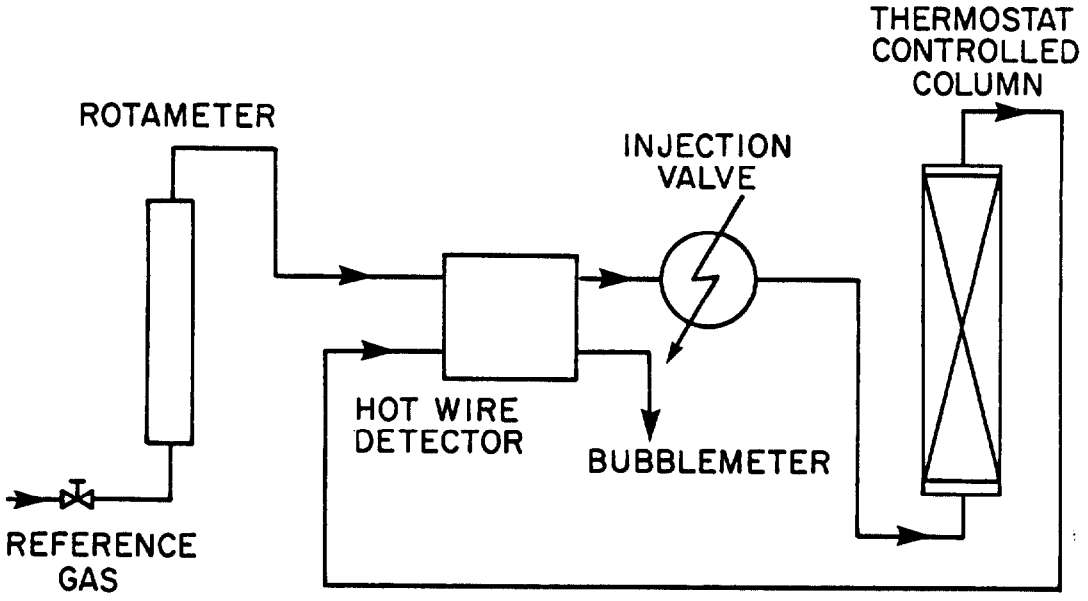

FIGURE 1
SCHEMATIC DIAGRAM OF THE APPARATUS

During initial dehydration of the adsorbent the column was placed in a thermostatically controlled tubular furnace at 400°C and purged with He carrier for a period of 36 hours. For the experimental measurements the column was immersed in a low-temperature thermostatic bath (Tamson LT-9 range 200 K - 298 K).

The adsorbent column was packed with 20-60 mesh ($R_p \sim 0.021$ cm) or 14-20 mesh ($R_p \sim 0.05$ cm) particles. Details of the adsorbents are given in Table II. Potassium chabazite was prepared from the natural (Ca) form by exchange with aqueous KCl solution at 75°C for a period of 48 hours. The de-aluminated mordenite sample was prepared by acid leaching according to the method of Chen and Smith[32].

Results and Discussion

First and second moments were calculated from the experimental chromatograms according to eqs. (3) and (4). For weakly adsorbed species such as He (and N_2 at the higher temperatures) the retention time in the adsorption column is short. Under these conditions it becomes

Table II. Details of adsorbents

Adsorbent	Source Properties
4A	Union Carbide, 20-60 mesh ($R_p \approx 0.021$ cm)
Natural Chabazite	From Bowie, Arizona, supplied by Minerals Research of Clarkson, N.Y. Product no. 27112, 20-60 mesh. Mole Ratio $CaO:Na_2O:K_2O$ = 1.0:0.72:0.15
K-Chabazite	Prepared from natural chabazite by ion exchange with aqueous KCl at 75°C for 48 hours, 20-60 mesh. Mole Ratio $Cao:Na_2O:K_2O$ = 0.02:0.01:1.0
Erionite	From Shoshone, California, supplied by Minerals Research of Clarkson, N.Y. 20-60 mesh, Product no. 27102
Clinoptilolite	From Hector, California, supplied by Minerals Research of Clarkson, N.Y. 20-60 mesh. Product no. 27022
Animal Charcoal	From BDH Chemicals Ltd., Poole, England. Product No. 33030, used a crushed portion of 20-60 mesh size
Na-Mordenite	From Norton, Worcester, Massachusetts. Type 900, Lot No. 40155, obtained as 0.3 cm pellets, used as 20-60 mesh
H-Mordenite	From Norton, Worcester, Massachusetts. Type 900, Lot No. 40157, obtained as 0.3 cm pellets, used as 20-60 mesh and 14-20 mesh. Mole ratio $SiO_2:Al_2O_3$ = 1:0.097
De-aluminated H-Mordenite	Prepared from H-mordenite by leaching with HCl[32], 20-60 mesh. Mole ratio $SiO_2:Al_2O_3$ = 1:0.055

necessary to correct the measured first and second moments for the time delay and dispersion in the injection valve and detector system. The correction was determined in a series of measurements carried out with the column removed. For the more strongly adsorbed species the correction is negligible, although, for consistency it was applied throughout.

Equilibrium Data

Dimensionless equilibrium constants (Henry's Law constants) were calculated from the corrected first moments according to eq. (1). The results are summarized in Table III in which are listed the parameters K_o and ΔU giving the temperature dependence of the equilibrium constant according to the equation:

$$K_p = K_o \, e^{-\Delta U/RT} \qquad (11)$$

The data for H-mordenite, de-aluminated H-mordenite, erionite and chabazite are shown as vant Hoff plots in Figures 2 and 3.

Table III. Parameters K_o and ΔU giving temperature dependence of dimensionless equilibrium according to eq. (11)

System		$K_o \times 10^3$	$-\Delta U/R$ K
H-Mordenite (single expts.)	Kr	4.01	2660
	N_2	3.8	2300
H-Mordenite (mixture expts.)	Kr	5.3	2680
	N_2	10.3	2060
De-aluminated H-Mordenite	Kr	5.5	2580
	N_2	41	1590
Erionite	Kr	11.0	2200
	N_2	8.8	2100
K-Chabazite	Kr	270	1370
	N_2	38	1800
Natural Chabazite	Kr	23	2260
	N_2	3.5	2900
Clinoptilolite	Kr	61	1600
	N_2	390	1140
Animal Charcoal	Kr	15	1580
	N_2	64	1060

Most of the measurements were made by injecting either pure Kr or pure N_2 into the He carrier but in two series of runs a mixture containing 1% Kr in N_2 was used. Both kinetic and equilibrium parameters determined from the mixture experiments are consistent with the single component data.

Equilibrium isotherms for both Kr and N_2 on H-mordenite were also measured by an entirely independent gravimetric method on a Cahn vacuum microbalance system. The gravimetric and chromatographic data are compared in Figure 4 and it is evident that there is good agreement.

For an equilibrium-based adsorption separation process the most important parameter is the selectivity ratio α. A comparison of the α values for the adsorbents examined in the present study is shown in

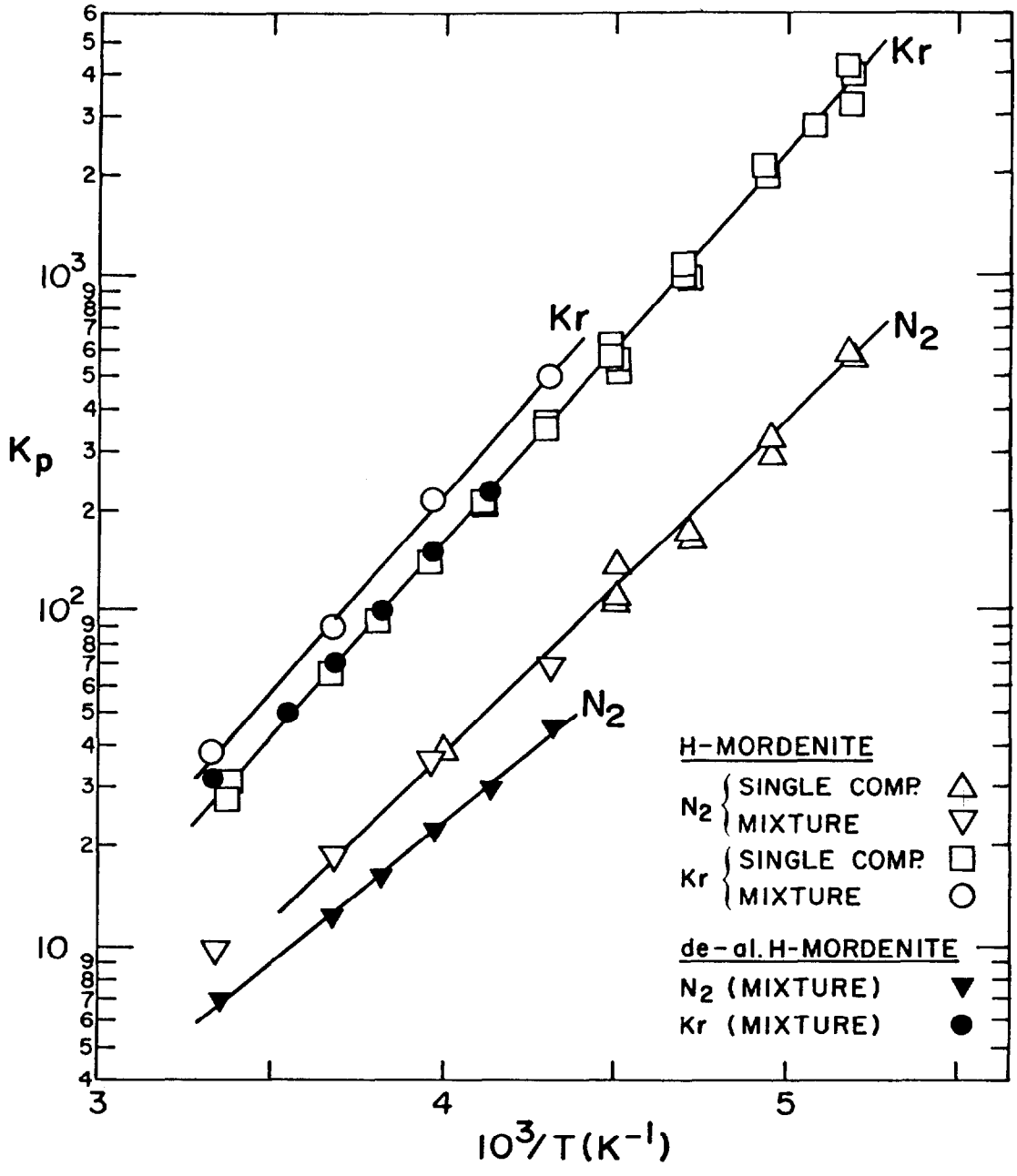

FIGURE 2
VANT HOFF PLOT SHOWING TEMPERATURE DEPENDENCE OF ADSORPTION EQUILIBRIUM CONSTANTS FOR N_2 AND Kr ON H-MORDENITE AND DE-ALUMINATED H-MORDENITE

Figure 5. It is clear that H-mordenite, particularly in de-aluminated form, is the best of the zeolitic adsorbents so far examined. The selectivity is comparable with the best activated carbon adsorbents and a modest extrapolation of the data suggests that at temperatures below 200 K the selectivity of de-aluminated H-mordenite becomes even greater than that of activated carbon.

A comparison between the data for H-mordenite and for de-aluminated H-mordenite shows that the enhanced selectivity of the de-

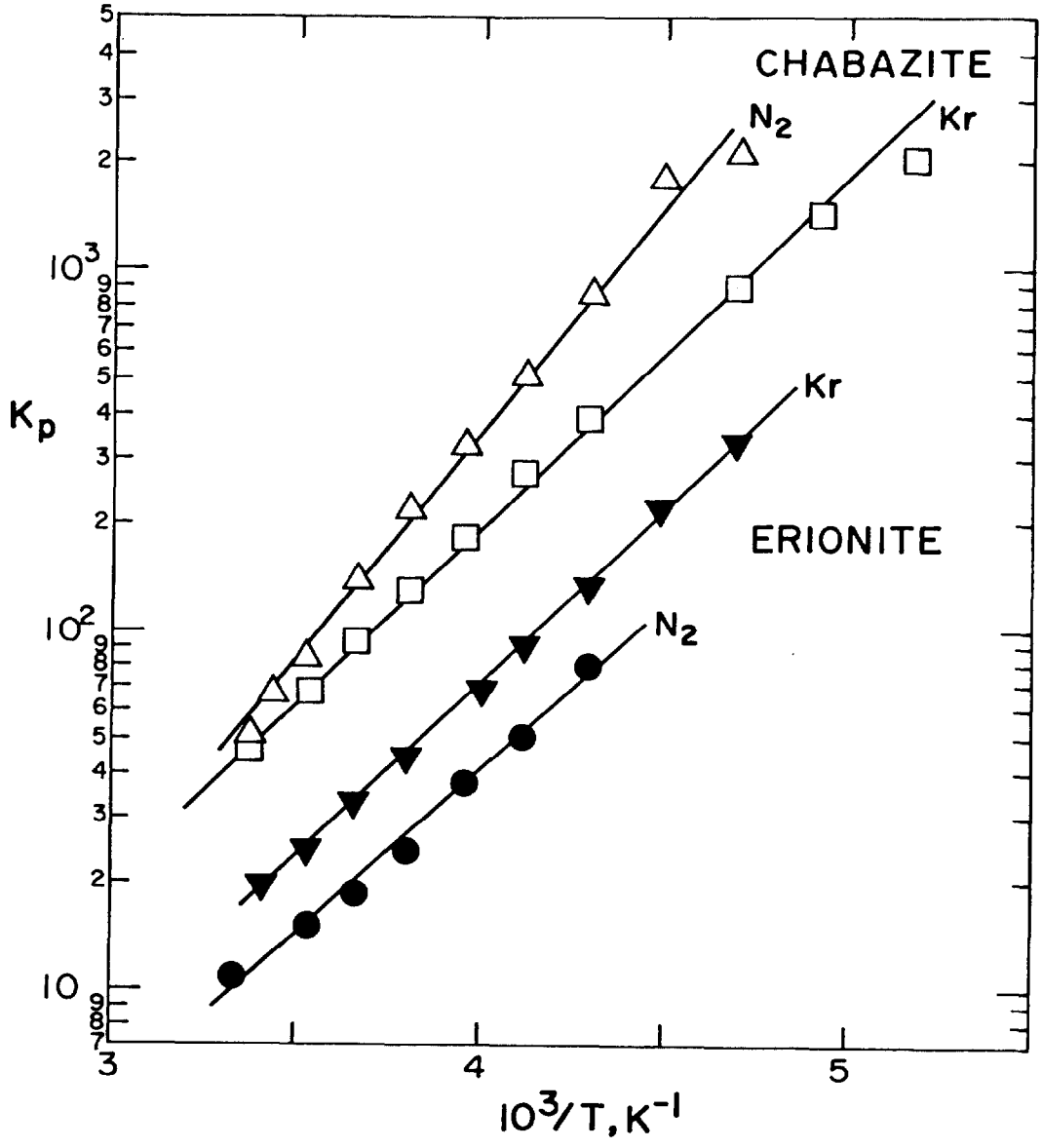

FIGURE 3
VANT HOFF PLOT SHOWING TEMPERATURE DEPENDENCE OF ADSORPTION EQUILIBRIUM CONSTANTS FOR N_2 AND Kr ON ERIONITE AND NATURAL CHABAZITE

aluminated form is due to a decrease in the affinity for N_2 rather than to enhanced adsorption of Kr. This behaviour is consistent with theoretical expectation since reduction of aluminum content leads to a reduced electrostatic field within the crystal and a corresponding decrease in the energy of interaction for the quadrupolar nitrogen molecule. Some further increase in selectivity might be achieved by further de-alumination since it is possible to increase the SiO_2/Al_2O_3 ratio to about 60 without de-stabilizing the mordenite structure.

The small apparent difference between the selectivity of H-mordenite as determined from separate Kr and N_2 data and from the mixture experiments is probably not significant since the individual equilibrium constants for N_2 and Kr from the single component and

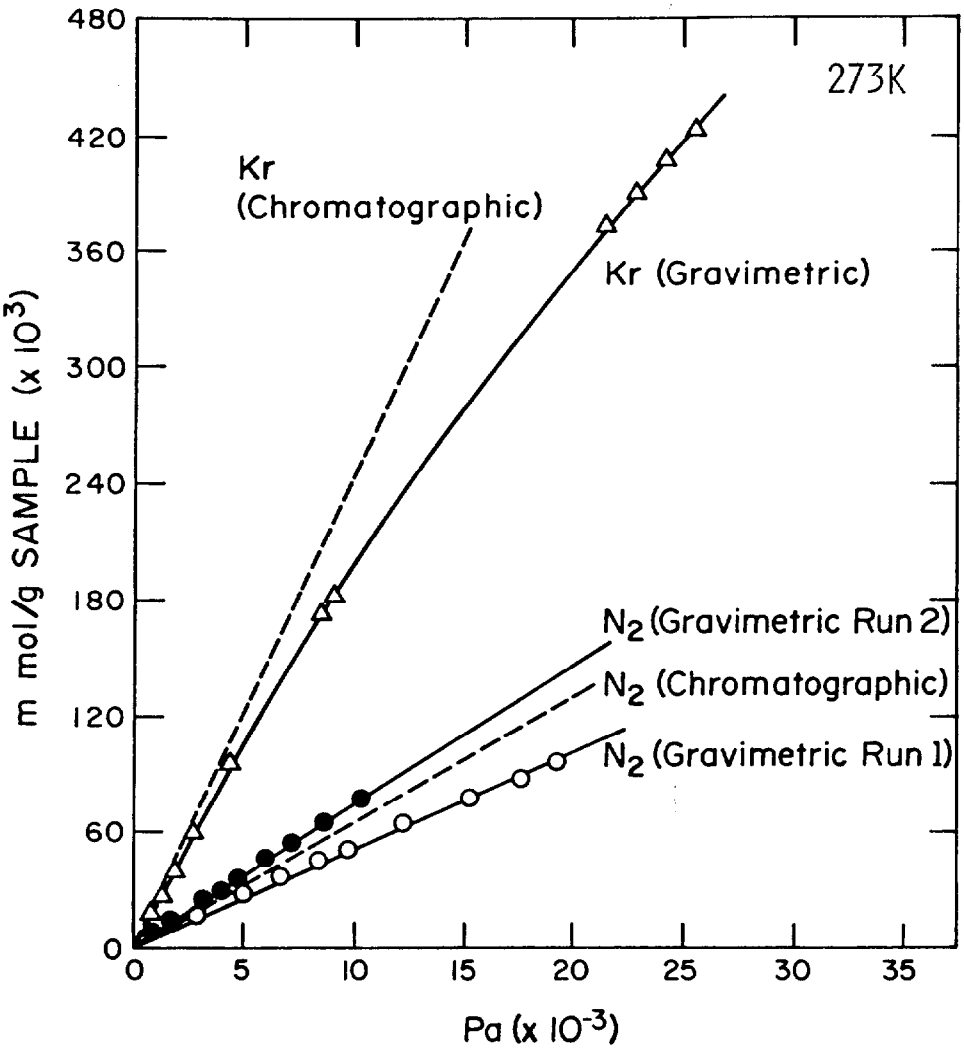

FIGURE 4
COMPARISON OF GRAVIMETRIC AND CHROMATOGRAPHIC EQUILIBRIUM DATA FOR Kr AND N_2 ON H-MORDENITE

mixture experiments are consistent within the limits of experimental error. The chromatographic separation of the Kr-N_2 mixture is illustrated in Figure 6. The increased resolution at the lower temperature is clearly apparent.

Kinetic Data

The results of some of the axial dispersion measurements performed with a He pulse are summarized in Figure 7 which shows $\sigma^2 L/2\mu^2 v$ plotted against $1/v^2$. In the low Reynolds number region D_L is approximately independent of gas velocity and, for He, the mass transfer resistance is negligible. It follows from eq. (6) that the plot of $\sigma^2 L/2\mu^2 v$ vs. $1/v^2$ should approximate a straight line through the origin with slope D_L. Although there is considerable scatter the experimental data show approximately this behaviour. The values of D_L estimated from the slope are similar to although somewhat larger than the theoretical values estimated according to eq. (8). Experiments

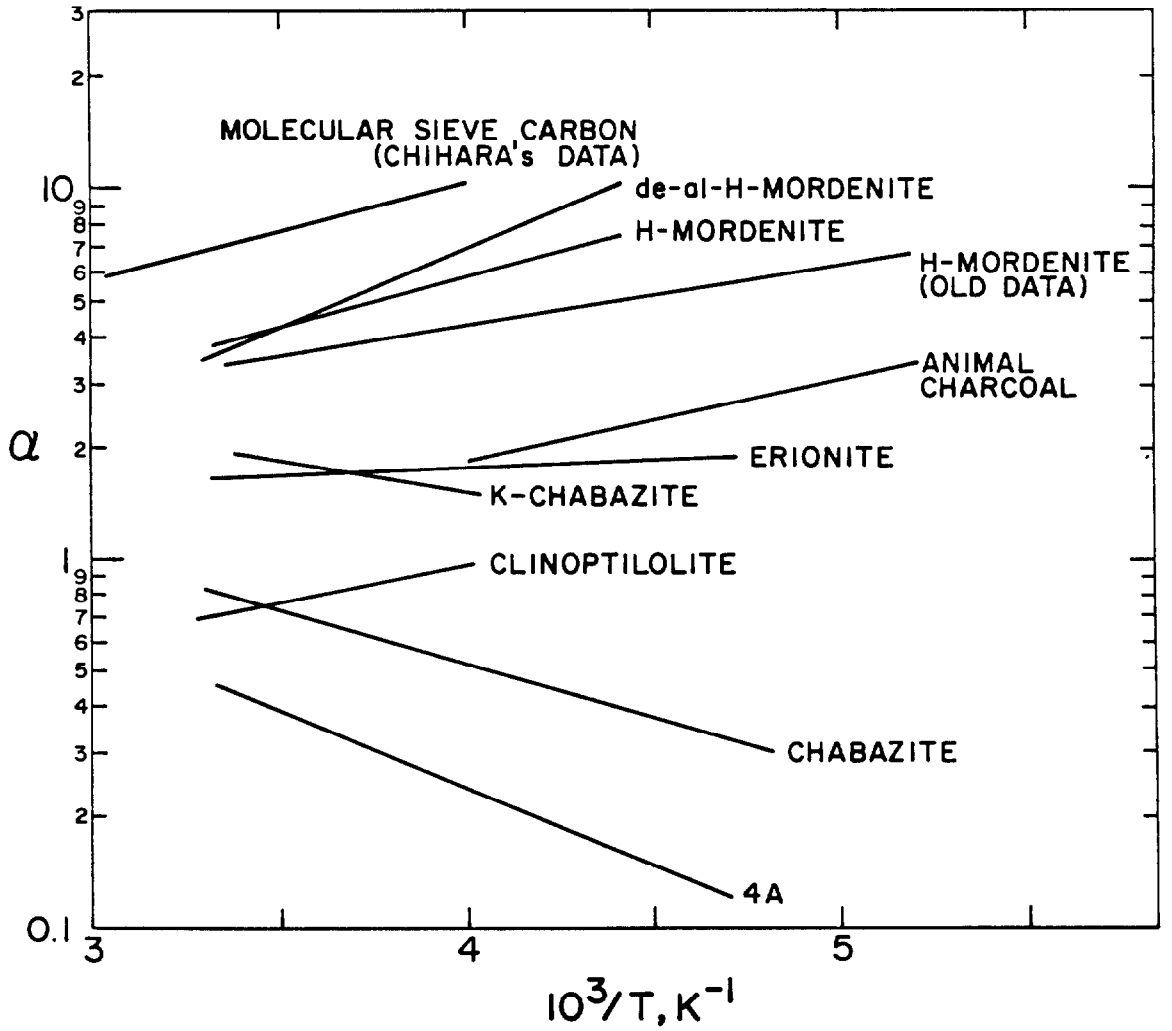

FIGURE 5
TEMPERATURE DEPENDENCE OF EQUILIBRIUM SELECTIVITY
$\alpha = (K_p)_{Kr}/(K_p)_{N_2}$ FOR VARIOUS ADSORBENTS

with H-mordenite at 298 K were performed with two different adsorbent particle sizes (R_p = 0.021 and 0.05 cm). The results, shown in Figure 7, indicate no significant variation in dispersion with particle size, as is to be expected in the low Reynolds number regime.

Figure 7 shows also the dispersion data for Kr and N_2 in H-mordenite at three different temperatures. It is evident that the curves for Kr lie close to the axial dispersion limit, as measured by the He curves, showing that the mass transfer resistance for Kr is too small to measure. This is seen to be true for both particle sizes. By contrast for N_2 the dispersion is considerably greater than for He or Kr indicating that mass transfer resistance is significant. The external film and macropore resistance $(\varepsilon/(1-\varepsilon))(1/3 + \tau/150)(D_p/R_p^2)$, which can be estimated with some confidence, is very much smaller than the difference $\sigma^2 L/2\mu^2 v - D_L/v^2$ so one may conclude that the main resistance to mass transfer in this system is intracrystalline diffusion. The diffusional time constants (D_c/r^2) for N_2, calculated from the

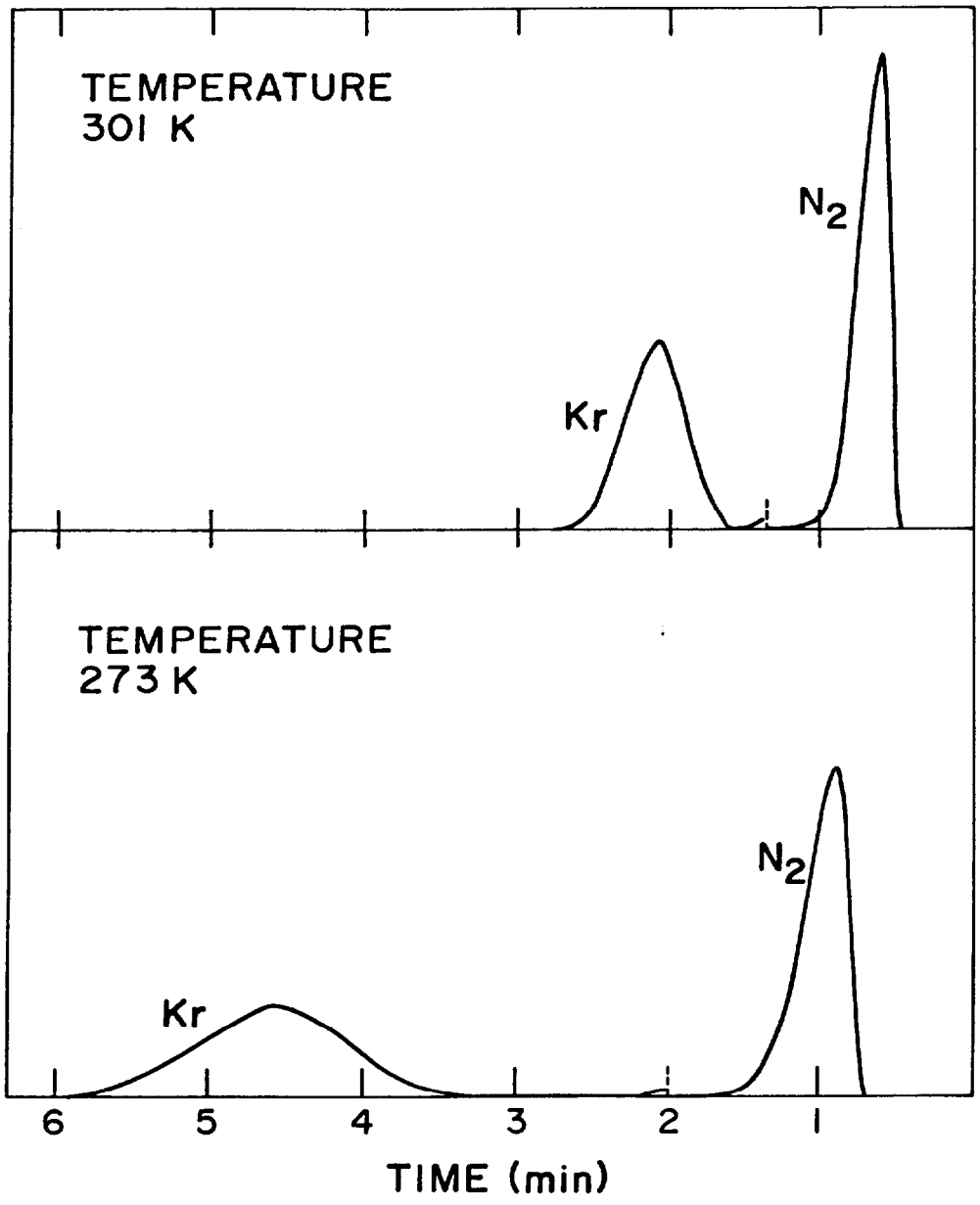

FIGURE 6
CHROMATOGRAMS MEASURED FOR 1.0% Kr IN N_2 MIXTURE WITH DE-ALUMINATED H-MORDENITE AS ADSORBENT SHOWING DIRECTLY THE INCREASE IN SELECTIVITY AND RETENTION TIME WITH DECREASING TEMPERATURE. Kr PEAKS WERE RUN AT 160 TIMES THE SENSITIVITY USED FOR N_2 PEAKS. EXCEPT FOR THE TEMPERATURE THE EXPERIMENTS WERE RUN UNDER IDENTICAL CONDITIONS.

difference $\sigma^2 L/2\mu^2 v - D_L/v^2$, are shown in Figure 8. There is considerable scatter in the data but the order of magnitude and the trend with temperature are clearly evident.

In some of the other systems the mass transfer resistance was greater making diffusivities easier to measure. The results for several adsorbents are summarized in the form of Arrhenius parameters in Table IV. In most of the adsorbents N_2 diffuses faster than Kr but in

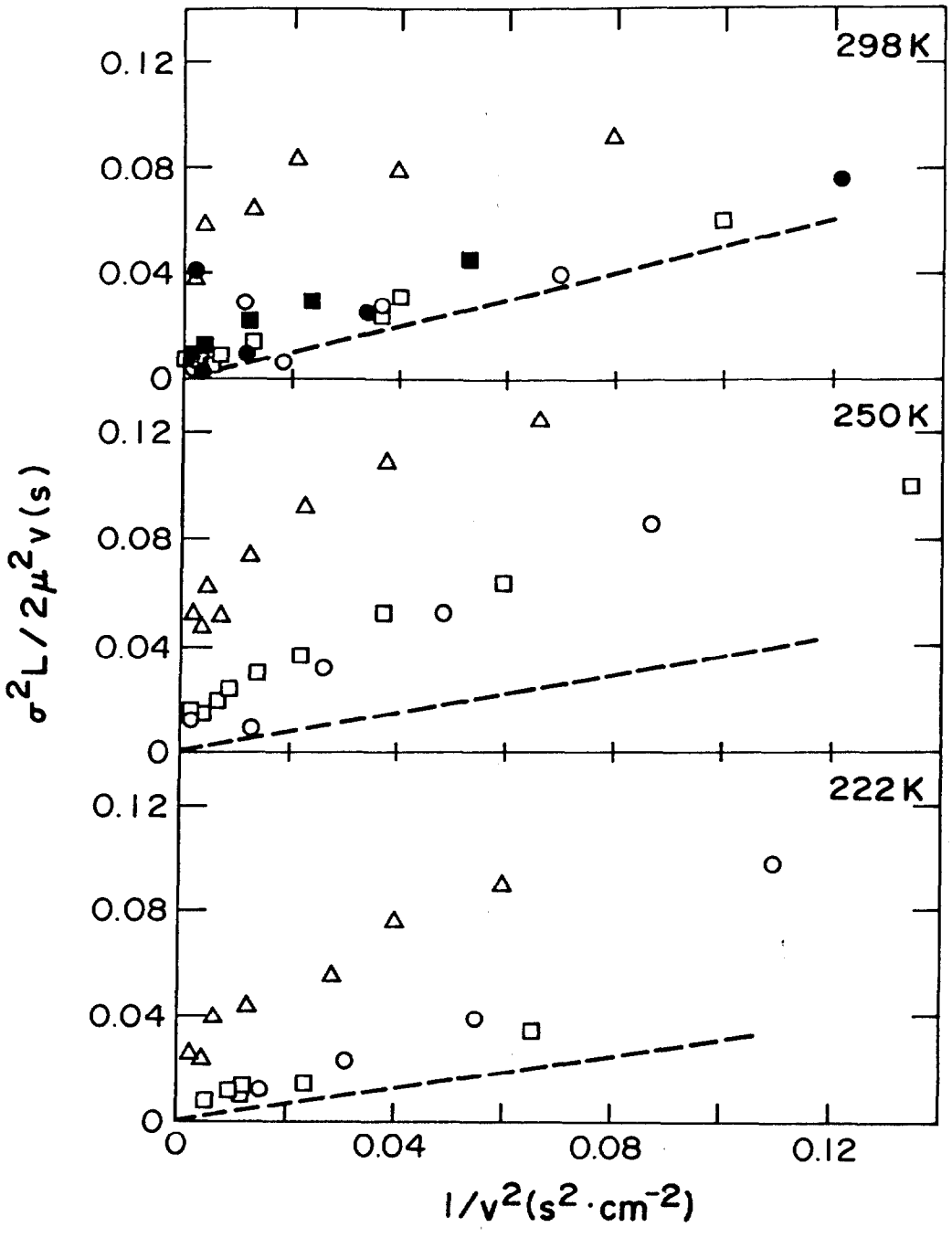

FIGURE 7
VARIATION OF $(\sigma^2/2\mu^2)(L/v)$ WITH $1/v^2$ FOR N_2 (Δ), Kr (■,□) AND He (●,○) IN H-MORDENITE. FILLED SYMBOLS (■,●) REFER TO 14-20 MESH, OPEN SYMBOLS ARE FOR 20-60 MESH PARTICLES. COLUMN LENGTH = 11.43 cm. THE LIMITING LINES CALCULATED ASSUMING $D_L = 0.7\ D_m$ ARE ALSO SHOWN (-----)

both H-mordenite and natural chabazite Kr is the faster diffusing species. The results for chabazite, which are shown in Figure 9, show the important role played by the exchangeable cation. It may be seen that in the natural (Ca) chabazite Kr diffuses faster than N_2 but in the potassium-exchanged form this order is reversed.

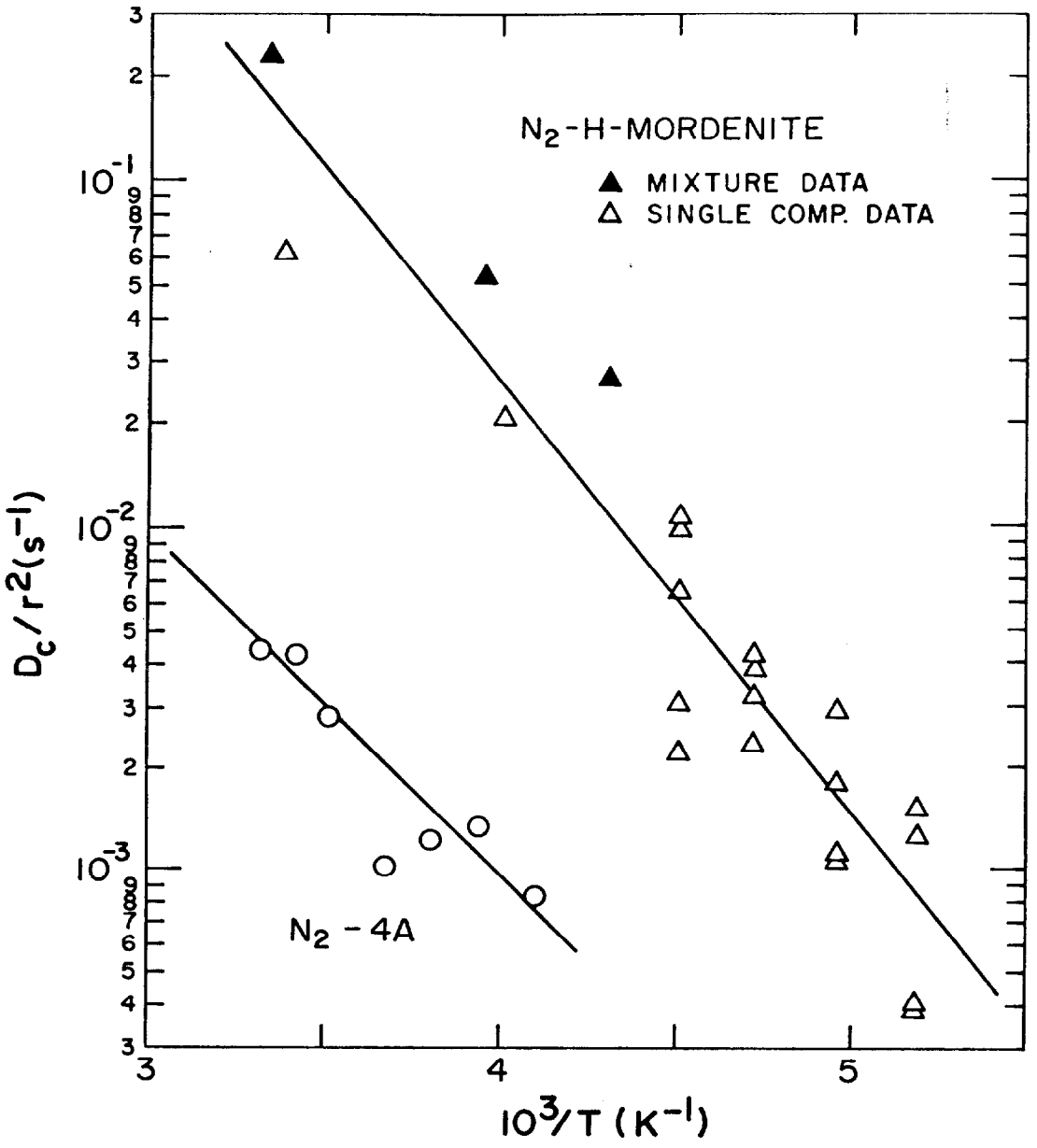

FIGURE 8
ARRHENIUS PLOT SHOWING TEMPERATURE DEPENDENCE OF DIFFUSIONAL TIME CONSTANT FOR N_2 IN H-MORDENITE AND 4A SIEVE

The difference in the diffusional activation energies for Kr and N_2 in natural chabazite is about 15 kJ/mol. At low temperatures ($\sim$ 200 K) this leads to an order of magnitude difference in the diffusivities and such a difference may be sufficiently large to provide the basis for a kinetic separation.

The kinetic selectivity of H-mordenite could not be quantitatively determined because diffusion of Kr was too fast to measure with any confidence. The results show that Kr is adsorbed more rapidly than N_2 but we cannot at present say whether the difference in diffusivity is large enough to allow a kinetic separation.

Table IV. Arrhenius parameters giving temperature dependence of zeolitic diffusivity according to $D_c = D_o e^{-E/RT}$

Sieve	Sorbate	E/R K	D_o/r^2 s^{-1}
Natural Chabazite	N_2	4.5	6×10^4
	Kr	2.6	230
K-Chabazite	N_2	2.5	75
	Kr	1.0	0.072
H-Mordenite	N_2	2.9	2.3×10^3
Clinoptilolite	Kr	6.5	1.2×10^8
4A Sieve	N_2	2.3	10
	Comparative Gravimetric Data		
4A Sieve	N_2	2.8 - 3.1	D_o* = 1 - 13 x 10^{-6} $cm^2 \cdot s^{-1}$
	Kr	4.1	$D_o = 10^{-7}$ $cm^2 \cdot s^{-1}$

* A detailed study of diffusion of N_2 in several different samples of 4A zeolite showed consistent activation energies but large differences in D_o[33].

Conclusion

The chromatographic method has been shown to provide a simple method for screening of adsorbents. In order to derive reliable kinetic data from the chromatograms it is necessary to allow for the effect of axial dispersion, and the required correction may be found by measuring the dispersion of a He pulse in a carrier of the more strongly adsorbed species (N_2). Both the kinetic and equilibrium data derived from the chromatographic experiments are shown to be consistent with the results of independent gravimetric measurements, thus confirming the validity of the method.

Of the adsorbents examined the most promising for selective removal of Kr by an equilibrium-based process is H-mordenite and it has been shown that the selectivity of this adsorbent increases with increasing Si/Al ratio. This adsorbent also has the advantage that diffusion rates are relatively high and the intracrystalline diffusivity of Kr is greater than that of N_2. This means that by judicious design of the adsorption process cycle it should be possible to take advantage of the difference in diffusion rate to enhance the selectivity for Kr.

At low temperatures Kr also diffuses faster than N_2 in natural chabazite but this adsorbent appears to be less attractive than H-mordenite since the equilibrium selectivity for Kr is lower.

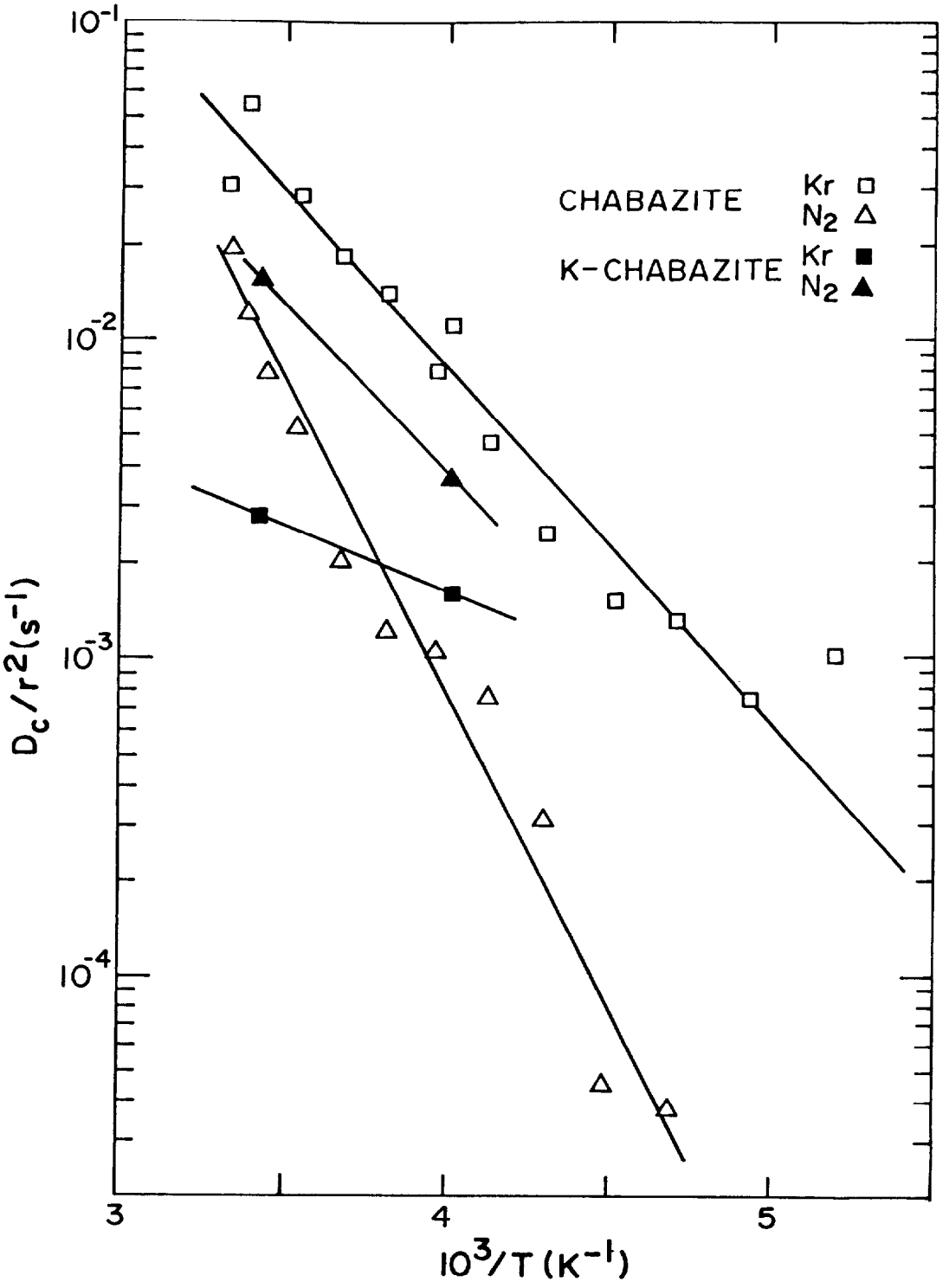

FIGURE 9
ARRHENIUS PLOT SHOWING TEMPERATURE DEPENDENCE OF DIFFUSIONAL TIME CONSTANTS FOR N_2 AND Kr IN NATURAL CHABAZITE AND K-CHABAZITE

Acknowledgement

We are grateful to Mr. Haldun Tezel for carrying out the gravimetric equilibrium measurements.

Notation

c	sorbate concentration in gas phase
D_c	diffusivity within a zeolite crystal
D_L	axial dispersion coefficient
D_m	molecular diffusivity
D_o	pre-exponential factor in equation in Table IV
D_p	macropore diffusivity (based on free pore area)
E	diffusional activation energy
$-\Delta H$	limiting heat of adsorption
$-\Delta U$	limiting internal energy of adsorption ($\Delta U = \Delta H + RT$)
k	external film mass transfer coefficient
K_p	adsorption equilibrium constant based on sorbate concentration in a pellet of sieve
K_o	pre-exponential factor in eq. (11)
L	length of chromatographic column
r	radius of zeolite crystal
R	gas constant
R_p	pellet radius
t	time
v	interstitial fluid velocity

Greek Letters

α	equilibrium selectivity $\equiv (K_p)_{Kr}/(K_p)_{N_2}$
Θ	porosity of pellet
ε	void fraction of bed
μ	first moment of response peak (defined by eq. (3))
σ^2	second moment of response peak (defined by eq. (4))
τ	tortuosity factor

References

1. Keilholtz, G.W., "Kr-Xe removal systems", Nuclear Safety 12(6), 591 (1971).

2. Slansky, C.M., "Separation processes for noble gas fission products from off-gas of fuel re-processing plants", Atomic Energy Reviews 9, 423 (1971).

3. Bendixsen, C.L. and Knecht, D.A., "Separation and storage of Kr", Int. Symp. on Management of Wastes from LWR Fuel Cycles, Conf-760701, 343 (1976).

4. de Bruijn, H., Gruetter, A., Roemberg, E., Shorrock, J.C., Werner, L. and Wood, F.C., "Removal of fission product noble gases from He of the HTGR using charcoal at low temperature", Trans. Inst. Chem. Eng. 42, T365 (1964).

5. Adams, R.E., Browning, W.E. and Ackley, R.D., "Containment of radioactive fission gases by dynamic adsorption", Ind. Eng. Chem. 51(2), 1467 (1959).

6. Kanazawa, T., Soya, M., Tanabe, H., An, B., Yuasa, Y., Ohta, M., Watanabe, A., Nagao, H., Tani, A. and Mikarada, H., "The cryogenic selective adsorption-desorption process for removal of radioactive noble gases", 14th ERDA Air Cleaning Conference Vol. II (1976), CONF-760822-V2, 964 (1976).

7. Pence, D.T., Chou, C.C., Christian, J.D. and Paplawsky, W.J., "Noble gas separation with the use of inorganic adsorbents", 15th DOE Nuclear Air Cleaning Conference, CONF-780819-P1, 512 (1979).

8. Forsberg, C.W., "Separation of Kr and Xe from CO_2 + O_2 with molecular sieves", Oak Ridge National Laboratories Report, ORNL/TM-5826 (1977).

9. Armond, J.W., "Practical application of pressure swing adsorption to air and gas separation", Symposium on Properties and Applications of Zeolites, 1979 April. Proceedings - Special Publication No. 33, The Chemical Society, London, 1980.

10. Drinkard, B.M., Allen, P.T. and Unger, E.H., "Gas chromatographic separation of C_8 aromatic mixtures", U.S. Pat. 3656278 (1972).

11. Ackley, R.D. and Browning, W.E., "Equilibrium adsorption of Kr and Xe on activated carbon and Linde molecular sieves", ORNL-CF-61-2-32 (ORNL report) (see also reference 5).

12. Kitani, S. and Takada, J., "Adsorption of Kr and Xe on various adsorbents", J. Nucl. Sci. Technol. (Japan) 2(2), 51 (1965).

13. Chihara, K., Suzuki, M. and Kawazoe, K., "Adsorption rates on molecular sieving carbon by chromatography", AIChE J. 24, 237 (1978).

14. Barrer, R.M., Papadopoulos, R. and Ramsay, J.D.F., "Sorption of Kr and Xe in zeolites at high pressure and temperatures", Proc. Roy. Soc. A326, 315 and 331 (1972).

15. Ruthven, D.M. and Derrah, R.I., "Diffusion of monatomic and diatomic gases in 4A and 5A zeolites", J. Chem. Soc., Faraday Trans. I 71, 2031 (1975).

16. Bosacek, V., "Gas chromatographic separation and adsorption of noble gases, oxygen and nitrogen on type X zeolites", Coll. Czech. Chem. Commun. 29, 1797 (1964).

17. Barrer, R.M. and Davies, J.A., "Sorption in decationated zeolites", Equilibrium data for Xe, Kr and N_2 in H-chabazite over temperature range 144-220 K, Proc. Roy. Soc., A320, 289 (1970).

18. Takaishi, T., Yusa, A. and Amakasu, F., "Sorption of N_2, O_2 and Ar on mordenite", J. Chem. Soc., Faraday Trans. I 67, 3565 (1971).

19. Lee, Lap-Keung and Ruthven, D.M., "Analysis of thermal effects in adsorption rate measurements", J. Chem. Soc., Faraday Trans. I 75, 2406 (1979).

20. Haynes, H.W., "Determination of effective diffusivity by gas chromatography. Time Domain Solutions", Chem. Eng. Sci. 30, 955 (1975).

21. Sarma, P.N. and Haynes, H.W., Application of gas chromatography to measurements of diffusion in zeolites", Adv. Chem. Ser. 133, 205 (1974).

22. Haynes, H.W. and Sarma, P.N., "A model for the application of gas chromatography to measurements of diffusion in bidisperse catalysts", AIChE J. 19, 1043 (1973).

23. Shah, D.B. and Ruthven, D.M., "Measurement of zeolitic diffusivities and equilibrium isotherms by chromatography", AIChE J. 23, 804 (1977).

24. Gangwal, S.K., Hudgins, R.R., Bryson, A.W. and Silveston, P.L., "Interpretation of chromatographic peaks by Fourier analysis", Can. J. Chem. Eng. 49, 113 (1971).

25. Scott, D.S., Lee, W. and Papa, J. "Measurement of transport coefficients in gas-solid heterogeneous reactions", Chem. Eng. Sci. 29, 2155 (1974).

26. Boersma-Klein, W. and Moulijn, J.A., "Evaluation in time domain of mass transfer parameters from chromatographic peaks", Chem. Eng. Sci. 34, 959 (1979).

27. Chou, T.S. and Hegedus, L.L., "Transient diffusivity measurements in catalyst pellets with two zones of differing diffusivities", AIChE J. 24, 255 (1978).

28. Ostergaard, K. and Michelsen, M.L., "On the use of the imperfect tracer pulse method for determination of hold-up and axial mixing", Can. J. Chem. Eng. 47, 107 (1969).

29. Edwards, M.F. and Richardson, J.F., "Gas dispersion in packed beds", Chem. Eng. Sci. 23, 109 (1968).

30. Langer, G., Roethe, A., Roethe, K.P. and Gelbin, D., "Heat and mass transfer in packed beds - III axial mass dispersion", Int. J. Heat Mass Transfer 21, 751 (1978).

31. Habgood, H.W. and MacDonald, W.R., "Effect of micropores on peak shape and retention volume in gas - solid chromatography", Anal. Chem. 42, 543 (1970).

32. Chen, N.Y. and Smith, F.A., "Preparation of dealuminized mordenite", Inorg. Chem. 15, 295 (1976).

33. Yucel, H. and Ruthven, D.M., "Diffusion in 4A zeolite", J. Chem. Soc., Faraday Trans. I 76, 60 (1980).

DISCUSSION

UNDERHILL: Working with Dr. Grubner at Harvard, I have been using moment analysis to analyze the interparticle diffusion coefficients on charcoal, and there are, I would say, about five or ten references where the type of moment analysis you present here has been used earlier.

RUTHVEN: I did not present this analysis as my own original work.

UNDERHILL: The references are available if you want them.

RUTHVEN: I think I am familiar with the references. Of course, I was just presenting the results of the analysis. I hope I did not leave people with the impression that moment analysis is something that I had originated or even that those equations were mine.

UNDERHILL: The second point is that the Antoine equation is probably the best three-parameter equation for fitting vapor pressure with liquids. But if you prefer a van't Hoff equation, then you should not be after thermodynamic perfection.

RUTHVEN: Well, I am not after perfection, but actually, if you looked at your numbers, I suspect that they would fit a van't Hoff equation reasonably well.

UNDERHILL: The van't Hoff correlation can be tested easily--all the data are on punched cards--but I doubt that any improvement will be found.

PENCE: You indicated that you thought that the adsorption coefficient may cross over and may actually be better than activated charcoal at the lower temperatures. We have looked at this with some of the zeolites, as you mentioned. We did not observe this. On the other hand, I am not certain of the data for the charcoal. But in both situations, it appears that when you get down to low enough temperatures, say -140° to -160°C, the adsorption coefficient does bend over rather rapidly, and even more rapidly for the zeolite than for the charcoal. The data are correct; they do cross over. Whereas at room temperature, some charcoalswill be better; if you go lower,

the zeolites are better than the charcoal. And then you get to a certain point and it appears that the nitrogen adsorbs more rapidly in the zeolites than in the charcoal.

RUTHVEN: When you are looking at the dynamic adsorption coefficient, it is a bit more complicated because you have also to consider kinetic effects. I was referring to the Henry's Law constants which, if you like, determine the selectivity and capacity under static conditions. Unfortunately, the activated carbon data we have do not extend to low temperatures, but a modest extrapolation suggests that there is a crossover at about 200K. Below this temperature the selectivity for Kr on the best zeolitic adsorbents becomes higher than on activated carbon. I don't think one can make too strong a statement on this point. Perhaps one should just say that at about 200K the selectivities of the H-mordenite and the best activated carbons are similar.

PENCE: I do not challenge that because I think you are in the right order of magnitude, but I think the data are pretty fuzzy. For the charcoal, the only data I can find appear to start crossing over, but I do not know how rapidly.

STEADY STATE OPERATION OF THE FIRST CRYOGENIC COLUMN IN A KRYPTON SEPARATION SYSTEM

R. von Ammon, W. Bumiller, E. Hutter, and G. Neffe
Kernforschungszentrum Karlsruhe
Federal Republic of Germany

Abstract

Recent results obtained during the operation of the inactive test unit KRETA for the cryogenic separation of krypton from simulated reprocessing off-gases are presented. The first rectification column of this unit was modified by shortening its lower part from 18 to 8 practical plates and placing the feed point into the warmer, krypton-rich section. Two essential results were thus achieved: plugging by desubliming xenon was not observed even at xenon feed concentrations as high as 1 vol.-%; and, accumulation of oxygen was much lower than in the column version used previously, thus reducing the potential hazard by ozone formation drastically. The accumulation of methane, however, was found to be high, in agreement with calculations.

I. Introduction

The first cryogenic column of KRETA has been laid out for a pressure of 5 bar. During the first operation campaigns the point of feedgas entrance was placed approximately in the center of the column where the temperature was that of a boiling N_2 - 3% Ar mixture (95 K at 5 bar). This is shown schematically at the left side of fig. 1. We call this column version KRETA I. With a stationary temperature profile as indicated in the figure, crystallization (desublimation) of xenon from the gas phase was observed whenever the xenon concentration in the feed gas exceeded approximately 800 vol.-ppm[1], resulting eventually in plugging of the column and breakthrough of krypton at the column

head. As it turned out, the holes of the sieve plate above the feed-point got plugged by desubliming xenon. As a consequence, this column part was flooded.

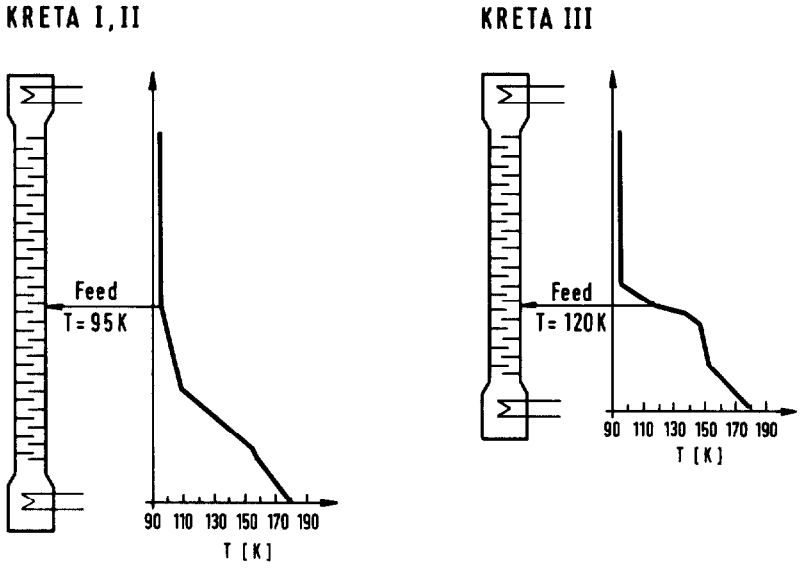

FIGURE 1 Feed Points and Temperature Profiles in KRETA Columns

Since the xenon concentration in the off-gas of the Wiederaufarbeitungsanlage Karlsruhe (WAK) at the peak of a fuel dissolution amounts to approximately 2000 vol.-ppm, and in the off-gas of a future large reprocessing plant is expected to be as high as 4000 vol.-ppm on an almost continuous level, this situation was not acceptable and had to be improved.

In addition, the accumulation of oxygen in the first column was found to be quite high[2]. In a radioactive off-gas system this may happen if traces of oxygen break through the pretreatment steps before the cryogenic section. Thus, the potential ozone hazard would pose rather stringent postulations on the effectiveness of the catalytic reduction step which is included in the off-gas treatment flowsheet

followed at Karlsruhe for the separation of oxygen and residual nitrogen oxides. This fact also called for an improved performance of the cryogenic unit by a modified version of the first column.

II. Modification of the First Column

1. Changes of Sieve Plates

An inspection of the sublimation pressure curve of xenon reveals the finding (fig. 2) that at 95 K desublimation of xenon should set in already at a xenon concentration of 50 vol.-ppm.

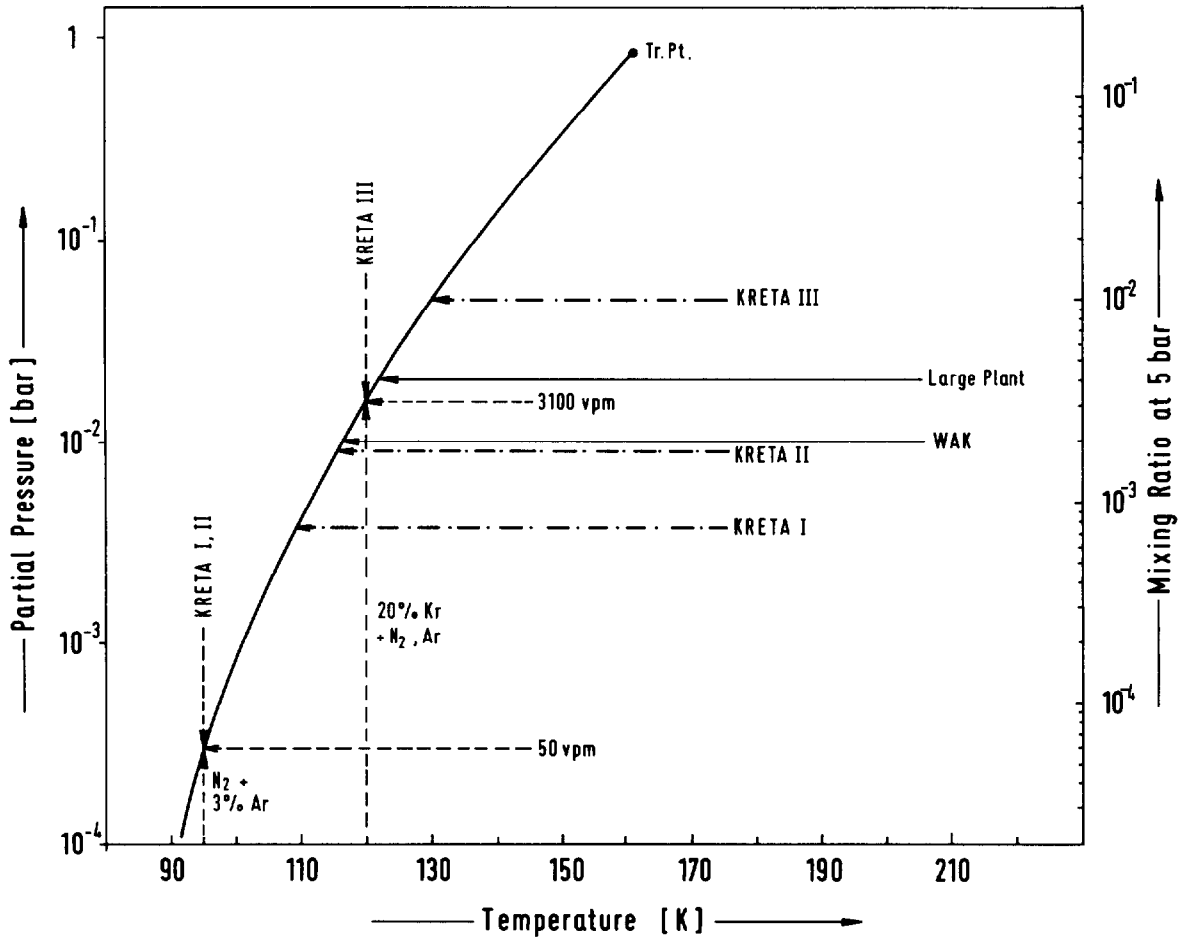

FIGURE 2 Sublimation Pressure of Xenon

Even considering that the xenon in the feedgas on entering the column is diluted somewhat by uprising vapor, it must be assumed that at a xenon concentration in the feedgas of 800 vol.-ppm the sublimation pressure curve is definitely exceeded and desublimation actually occurs. However, plugging of sieve holes does not take place because crystallizing xenon is carried down the column by the liquid and dissolved. Therefore, it was consequent to increase the hole diameter of the critical sieve plates above the feed point. In two experiments we replaced two sieve plates in this column section having holes with the usual diameter of 0.8 mm by plates with 2.0 mm and 5.0 mm holes, respectively. The hole number was reduced correspondingly to keep the active hole area constant. In this context this column version is called KRETA II.

2. Change of the Feed Point

The method just described cures only the symptoms, i.e. plugging of the column, but not their origin, i.e. desublimation of xenon. In order to eliminate the latter, the temperature in the vicinity of the feed point must be raised, so that the sublimation pressure of xenon is higher than or equal to its partial pressure in the gas mixture of feedgas and uprising gas in the column. For the xenon partial pressures in question this temperature should be around 120 K. This can be achieved by two methods: either by raising the operation pressure of the column or by placing the feed point into a warmer, krypton-rich column section.

For reasons of the type of the compressor available at the moment (water seal) we can raise the column pressure only up to six bar. The positive effect of increasing the pressure from four to six bar on the limiting xenon concentration in the feedgas was apparent, but not sufficient. For complete remedy of the xenon crystallization problem the operating pressure probably would have to be raised to approximately 20 - 25 bar.

So we chose to lower the feed point. Because the upper and lower parts of the column have a different gas/liquid ratio and therefore sieve plates with different hole numbers, it was not possible just to

shift the feedgas line. We simulated this by cutting out of the lower column part a section containing 10 plates. The feed point is now positioned eight plates above the reboiler (right side of fig. 1). In order to raise the temperature at this point, the krypton front must be raised from the fourth or fifth plate where it was usually held to the seventh plate. Thus a temperature of 120 K was reached at the feed point. It was held constant by controlling the power of the reboiler with a thermocouple at this point. This column version is now called KRETA III.

The krypton inventory is increased somewhat by this procedure, of course, but particular attention to the minimization of the inventory was not paid in the layout of this column. This will be done in a future version.

III. Results and Discussion

1. Desublimation of Xenon

The results of the various experiments are presented in table I and fig. 2.

Tabel I. Column parameters and xenon crystallization.

Column Version	Diameter of Sieve Holes above Feed Point	Temperature at Feed Point	Limiting Xe Concentration in Feed
I	0.8 mm	95 K	$\sim$ 800 vol.-ppm
II	2.0 mm	95 K	$\sim$ 1200 vol.-ppm
	5.0 mm	95 K	$\sim$ 1800 vol.-ppm
III	2.0 mm	120 K	$\geq$ 1 vol.-%

In table I only the variable parameters of influence to xenon crystallization are indicated. Other components of the feedgas were: Ar 1 vol.-%; Kr was always 1/10 of the xenon concentration, so that the concentration profiles of the steady state were not changed. The krypton concentration in the feedgas has no influence on the desub-

limation of xenon. The carrier gas was nitrogen.

Increasing the hole diameter of the two sieve plates above the feed point actually improved the column behavior as expected: with 2.0 mm holes instead of the usual 0.8 mm holes the limiting stationary xenon concentration was raised from 800 to 1200 vol.-ppm, and with 5.0 mm holes even to approximately 1800 vol.-ppm[3]. Thus, the maximum xenon concentration of the WAK off-gas was almost reached.

It is to be expected that the situation could be further improved by increasing the hole diameter still more, and that a limiting hole diameter could be reached, which cannot get plugged by desubliming xenon any more (fig. 3). In this case the thickness of the "ice" layer reaches a steady state where it is smaller than half the diameter of the hole. It is difficult to estimate this diameter because heat- and mass-transfer coefficients in this system are not known. Although the theory is available [4-6], their calculation is rather tedious and uncertain. In any case, a strong increase of the hole diameter would certainly influence the hydraulic properties of the plate. Therefore more than two plates had to be changed, in order not to just shift the desublimation problems into higher parts of the column.

This situation led us to abandon column version II and concentrate on type KRETA III with an altered feed point.

The results obtained with this column version are also presented in table I and fig. 2. Whereas the sublimation pressure of xenon at 120 K corresponds to a mixing ratio of 3100 vol.-ppm at 5 bar, we have fed xenon concentrations of up to 1 vol.-% into the column without any signs of plugging. 4000 vol.-ppm were run continuously during a 10-week campaign.

The rise of the krypton front in the column up to the vicinity of the feed point did not deteriorate the decontamination factor for the rare gases: it was still $\geq 10^3$ for krypton and $\geq 10^4$ for xenon as with the older column version. Its exact determination was limited by the sensitivity of the gas-chromatograph (0.1 vol.- ppm).

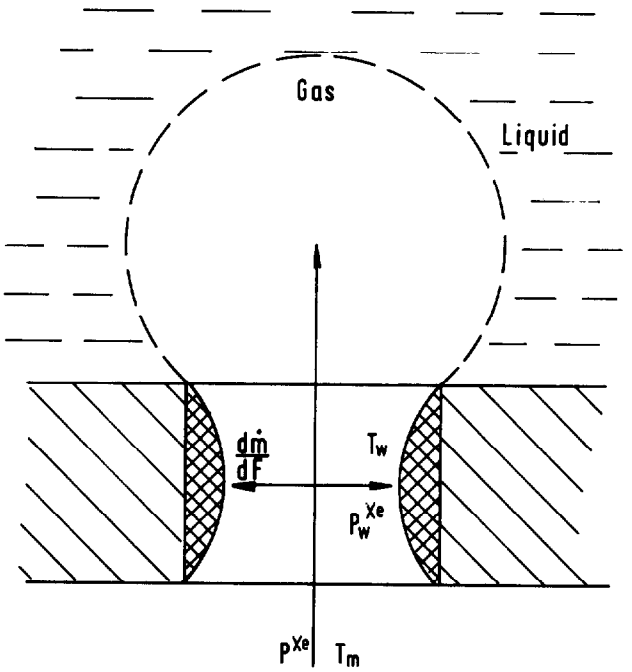

$$\frac{d\dot{m}}{dF} = \frac{\beta}{R\,T_m}\left(p^{Xe} - p_w^{Xe}\right)$$

$\frac{d\dot{m}}{dF}$	=	mass flow per unit area
β	=	mass transfer coefficient
T_m	=	temperature of gas phase
p^{Xe}	=	partial pressure of Xe in gas phase
T_w	=	temperature at wall or Xe frost surface
p_w^{Xe}	=	partial pressure of solid Xe

FIGURE 3
Desublimation of xenon in a sieve hole

In addition, the loss of 10 practical plates in the lower part of the column did not result in a serious increase of the concentrations of Ar and N_2 in the reboiler liquid. If this were the case, crystallization of xenon again could be caused, but now from the liquid phase[1,7]. Ar- and N_2-concentrations as measured in the liquid phase during steady state operation of the column were less than 50 vol.- ppm throughout.

2. Accumulation of Trace Impurities

2.1 Oxygen

The accumulation of O_2 which had been measured in the column during operation according to versions I and II was reported by us recently[2]. Analytical determinations of O_2 were carried out using electrochemical methods, either with an instrument working on ZrO_2-basis (Model DS 2000, Simac, Walton on Thames, Surrey, England) or an instrument working in alcaline solution (K. Gerhard, Blankenbach, Aschaffenburg, Germany). Sensitivity was $\leq$ 0.1 ppm and $\leq$ 1 ppm, respectively.

From fig. 4 can be seen, that in column versions I and II with an O_2-concentration of 10 vol.-ppm in the feedgas, an accumulation of up to 3 vol.-% in the gasphase of the seventh plate in the lower part of the column is obtained in satisfactory agreement with calculations.

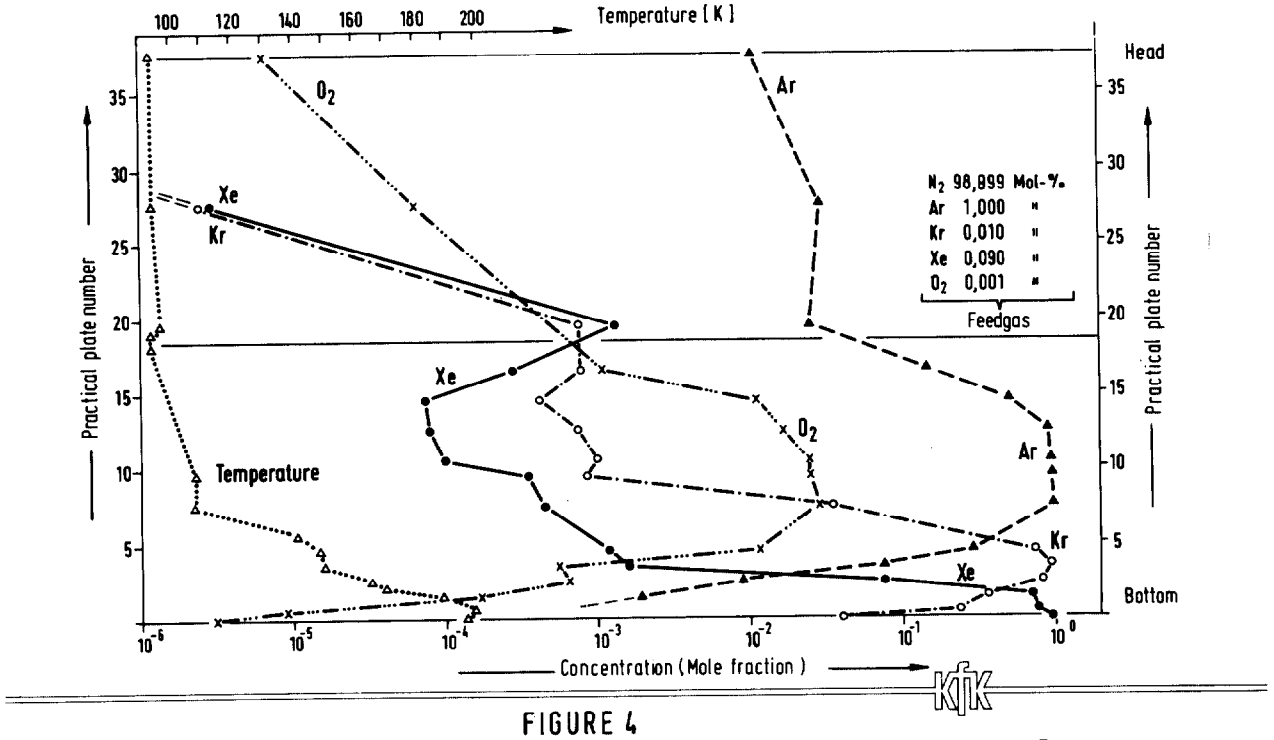

FIGURE 4
Experimental temperature- and concentration profiles in the first KRETA-column at 5 bar

In contrast, the O_2-concentration profile as measured in the column operated according to KRETA version III is quite different (fig. 5).

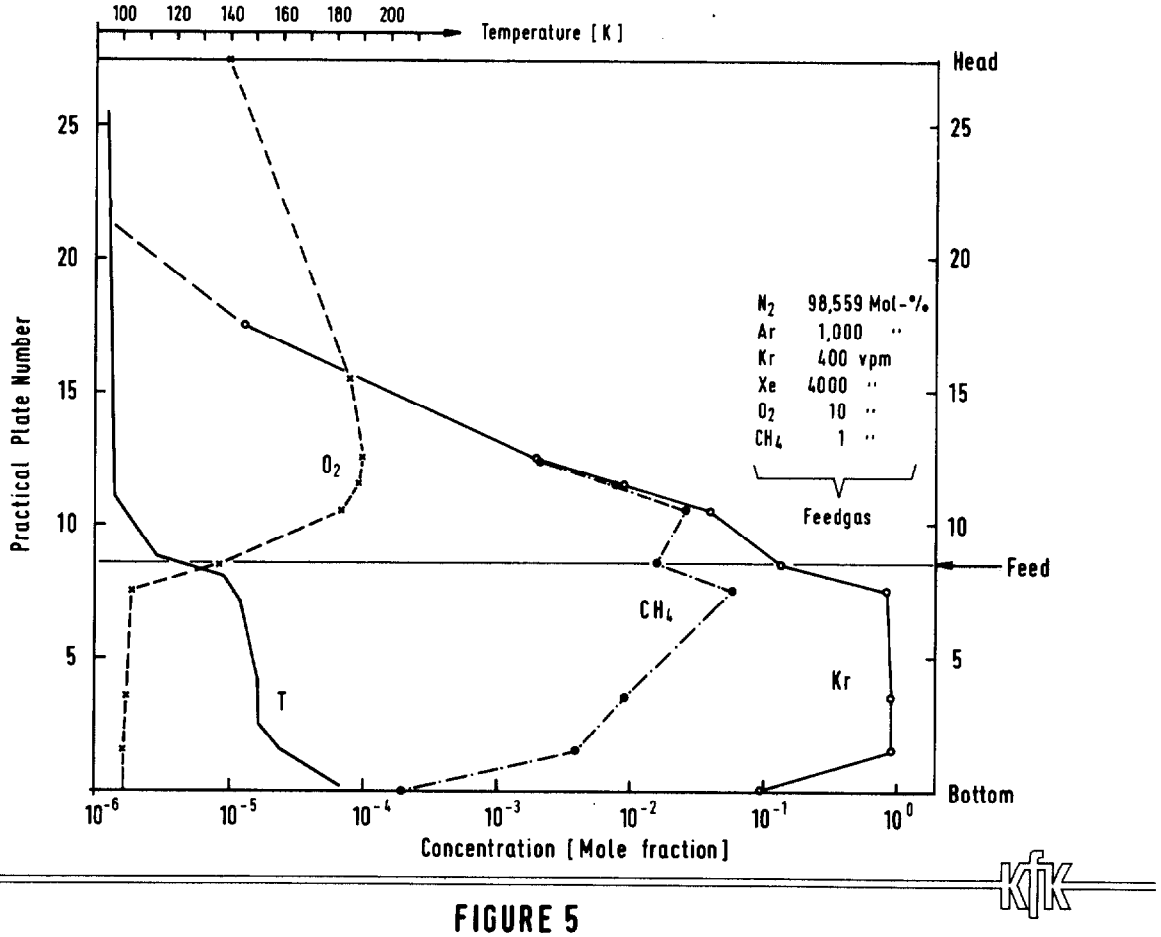

FIGURE 5

Temperature - and Concentration-Profiles in the Modified First KRETA Column

The maximum which is now a few plates above the feed point amounts to only 100 vol.-ppm. Thus, an enrichment factor of only 10 is obtained referred to the feed concentration of 10 vol.-ppm as compared to an enrichment factor of 3000 in the former case. Accordingly, the stationary state was approached much faster, i.e. after less than three days as compared to approximately 20 days. Except for a solubility in the reboiler liquid of about 1.5 ppm, O_2 is driven off completely at the column head.

It can be shown that at such a low O_2 level in the column, formation of ozone under radioactive conditions should be very low[8] and should not create a safety hazard.

2.2 Methane

Methane boils much closer to krypton than oxygen (table II).

Table II. Boiling points of off-gas components

Compound	Boiling point (K at 5 bar)
N_2	93.9
CO	98
Ar	105 7
O_2	108
CH_4	135
NO	139
Kr	144.9
Xe	199.2

It therefore accumulates near krypton in the first column and cannot be driven off at the column head. It will completely go to the reboiler liquid together with krypton and will thus reach the second column and the krypton product.

A concentration profile corresponding to a feed concentration of only 1 vol.-ppm as measured in the gasphase of a column operated according to KRETA version III is shown in fig. 5. This profile represents approximately the stationary state. Because of the high accumulation it would take an exceedingly long time to reach equilibrium with such a low feed concentration. We therefore fed at first a CH_4-concentration of 10 vol.-ppm into the column until we approximately had reached the concentrations calculated for 1 vol.-ppm CH_4 in the feedgas. Then we reduced the feed concentration to 1 vol.-ppm CH_4. After a total duration of 10 weeks the experiment was finished. In the equilibrium state the CH_4 amount leaving the column via the reboiler liquid must be equal to the CH_4 amount entering the column via the feedgas. This condition was approximately fulfilled:

the CH_4-concentration in the reboiler liquid was measured as 200 vol.-ppm, whereas 227 vol.-ppm were to be expected for a mixing ratio of Xe:Kr:CH_4 = 4000:400:1. The CH_4 analysis was carried out using gaschromatography with a flame ionization detector (sensitivity $\leq$ 0.5 vol.-ppm).

The maximum concentration at the accumulation point just below the feed point (7th plate) amounts to 6 vol.-% in the gas phase.

Although methane itself is not a very reactive substance, it may undergo radiolytic decomposition in the radiation field of Kr-85 and thereafter react with other impurities like O_2, O_3, or NO. It is difficult to assess at the moment the potential safety hazard of such reactions in a cryogenic krypton separation unit or in the krypton product. Therefore, very rigorous requirements have to be posed on the pretreatment steps to retain any CH_4 present in the off-gas and not to produce any new CH_4, e. g. from the reduction of CO_2 with H_2 at the reduction catalyst [2].

IV. Conclusions

After four years of operating experience with the inactive cryogenic test unit KRETA the following predictions can be made concerning the operability of such a system under real, radioactive conditions:

1. Crystallization of xenon presents no problem even at the relatively low pressure of 5 bar, if a feed point is chosen where the temperature is high enough. Although this is achieved by placing it in the krypton-rich column section, the decontamination factor of the column is still excellent.
2. Accumulation of oxygen in the first column is low under these conditions. Thus, the requirements for the effectiveness of O_2 separation in the pretreatment steps do not necessarily have to be rigorous, because ozone formation will be low.
3. There are, however, other impurities with boiling points close to

that of krypton which make the requirements for the pretreatment steps stringent, since they accumulate strongly in the first column and may give rise to radiolytic reactions. The most important of these components is methane.

References

1. R. von Ammon, H.-G. Burkhardt, E. Hutter, and G. Neffe, "Development of a cryogenic krypton-separation system for the off-gas of reprocessing plants", Proceed. 15th DOE Nuclear Air Cleaning Conf., Boston 1978, p. 640.

2. R. von Ammon, E. Hutter, and G. Knittel, "Catalytic redution of O_2 and NO_x - a critical pretreatment step for the cryogenic retention of Kr-85", Intern. Symp. on Management of Gaseous Wastes from Nuclear Facilities, Vienna 1980, IAEA-SM-245/12.

3. R. von Ammon, W. Bumiller, H.-G. Burkhardt, E. Hutter, and G.Neffe, "Die Entwicklung der Abtrennung von Kr-85 aus dem Abgas von Wiederaufarbeitungsanlagen", KfK-Nachrichten 11(3), 19(1979).

4. E.A. Rische, "Ausfrieren von Dämpfen aus Gas/Dampf-Gemischen bei erzwungener Rohrströmung", Chem.-Ing.-Techn. 9, 603 (1957).

5. H. Hausen, "Einfluß des Lewisschen Koeffizienten auf das Ausfrieren von Dämpfen aus Gas-Dampf-Gemischen", Chem.-Ing.-Techn. 7, 177 (148).

6. R.S. Eby, "The desublimation of krypton from a noncondensable carrier gas", Report K-1896 (Sept. 1978), Oak Ridge Gaseous Diffusion Plant.

7. R. von Ammon, H.-G. Burkhardt, E. Hutter and G. Neffe, "Trennung von Edelgasgemischen durch Tieftemperatur-Rektifikation: Entwicklung für die kerntechnische Abgasreinigung", Ber. Bunsenges. Phys. Chem. 83, 1143 (1979).

8. M.T. Dmitriev, O.I. Yurasova, and N.A. Koroleva, "Kinetics of radiochemical oxidation of nitrogen and ozone formation in large reaction volumes", J. Appl. Chem. (USSR) 43, 1952 (1970).